J. Condensed Matter Nucl. Sci. 17 (2015) 35–66

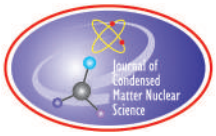

Research Article

Empirical Models for Octahedral and Tetrahedral Occupation in PdH and in PdD at High Loading

Peter L. Hagelstein*

Massachusetts Institute of Technology, Cambridge, MA 02139, USA

Abstract

High D/Pd loading is known to be a requirement for producing excess heat in the Fleischmann–Pons experiment, and much work has in recent years been focused on electrochemical protocols and cathode processing in order to achieve D/Pd loadings approaching unity routinely. However, we know very little about PdD at a loading near unity, and almost nothing about what happens when the loading exceeds unity. It may be that when the octahedral sites are fully occupied, additional interstitial deuterium atoms occupy tetrahedral sites, a proposal which at this point has little experimental support. It is nevertheless possible to construct an empirical model for this scenario, and to make use of available experimental data to fit the associated model parameters. We worked with empirical models for both PdD and PdH that assume an O-site energy quadratic in loading, and an O-site to T-site excitation which is either constant in loading, or else taken as an empirical function fit to estimates inferred from the analysis of experimental data. There are two empirical models, each with four or more free parameters; and insufficient experimental data from which to choose each parameter or function independently. We add supplementary constraints that presume the models for PdH and PdD must be very similar, which reduces the number of degrees of freedom within the models. This allows data from PdH to be used to construct a model for PdD, and vice versa. The models which result are interesting; they suggest these complicated systems might be understood based on a simple underlying picture; they indicate that there is more T-site occupation than has been appreciated previously in the literature; they indicate that the resistance ratio calibrations for PdH and PdD are inconsistent; and finally, measurements of the chemical potential at high loading have the potential to provide information about the O-site to T-site excitation energy.
 ISSN 2227-3123

Keywords: Empirical models, Resistance ratio, Solubility of PdH and PdD at high loading, Statistical mechanics model, Tetrahedral occupation

1. Introduction

We have been interested for many years in understanding the origin of the excess heat effect in the Fleischmann–Pons experiment, where a large amount of thermal energy is observed, with no commensurate chemical or energetic nuclear products observed [1,2]. We have long recognized that there must be new physical mechanisms involved, and along with many others we have put in much effort seeking to understand associated microscopic mechanisms [3,4]. Additionally,

*E-mail: plh@mit.edu

 ISSN 2227-3123

we have been interested in developing a simulation model for excess heat production, which involves a combination of known physics along with new physics. In this work our focus is on conventional physics issues connected with the octahedral and tetrahedral occupation of PdD at high loading.

It was understood by Fleischmann and Pons in 1989 that the D/Pd loading needed to be high in order for excess heat to be observed. Subsequently, two different loading requirements were identified. It was observed in experiments at SRI and ENEA Frascati that cathodes which did not reach a D/Pd loading in the vicinity of 0.95 at some point during their loading history were unlikely to produce excess heat [5–7]. For a cathode with did reach this very high loading, excess heat could be seen subsequently at more modest loading; however, excess heat was observed to increase with loading above a threshold in the vicinity of 0.83 [8–10].

Because of these observations, much attention has been focused on achieving high loading [11]; electrochemical protocols suitable for achieving high loading [12–16]; the problem of developing cathodes that can load well [14,15,17]; and materials science studies [18,19]. Measurements of the D/Pd loading can be done conveniently based on the resistance ratio [20–25], which has in recent years been determined to a D/Pd loading greater than unity. X-ray diffraction measurements have been reported [26–29], including measurements of samples loaded near unity [29].

This work has motivated our interest in some of the associated theoretical issues. For example, one might ask why there should be any requirements on the D/Pd loading in the first place. The question of what it is that happens in the experiment when the D/Pd loading reaches either 0.83 or 0.95 also come to mind [3,30,31]. Our interest in this work is focused on the deuterium chemical potential and site occupation when the D/Pd loading is in the vicinity of unity, or reaches even higher loadings.

From earlier experimental work, we know that hydrogen and deuterium atoms occupy interstitial octahedral sites in the FCC PdH or PdD lattice [32–35]. Such a picture is consistent with theoretical models that have been studied over the years [36–41]. The basic picture of highly loaded PdD at room temperature as an FCC lattice with NaCl-type structure, with deuterium atoms in the octahedral site (see Fig. 1), has provided one of the cornerstones for studies of PdH and PdD, and also for our field as well. Such a picture is useful as long as the tetrahedral occupancy is low; in this connection we draw attention to a calculation of the tetrahedral occupation as a function of pressure by Christensen et al. [40], which shows negligible tetrahedral occupation for D/Pd$<$1 even at very high pressure.

We are interested in the question of what happens when the D/Pd loading ratio exceeds unity, for example as has

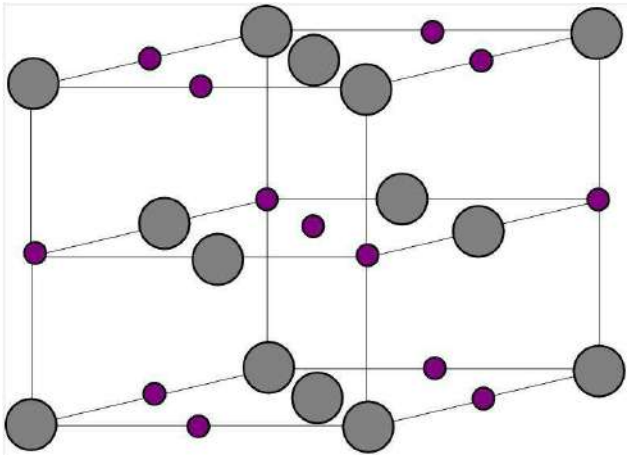

Figure 1. FCC lattice model for PdD; the large grey atoms in the figure are Pd, and the small purple atoms are D.

been claimed to have been achieved in high pressure experiments [42] up to 3.1 GPa. Note that there is not uniform agreement in the literature that the D/Pd loading can exceed unity under such conditions; for example, Hemmes et al. [43] models an H/Pd ratio less than unity for pressures up to 100 GPa. Sugimoto and Fukai model a variety of FCC metal hydrides up to 100 GPa, with no need for going above an H/Me ratio of unity [44].

However, if a D/Pd loading greater than unity can be achieved, then the question of where the extra deuterium atoms go in the lattice becomes important. Historically, this issue has largely been the focus of speculation. One possibility is that additional deuterium atoms occupy interstitial tetrahedral sites, once all of the octahedral sites are occupied [45–48]. Another suggestion is that double occupancy of octahedral sites occurs [49,50]. Such a suggestion seems unlikely since we would expect the occupation of anti-bonding orbitals which would tend to push the deuterium atoms apart [40] (although in the presence of a Pd vacancy this issue is removed [31]). In what follows, we examine simple models for tetrahedral occupation both for a D/Pd ratio less than unity as well as for D/Pd greater than 1.

Palladium vacancies become stabilized at high H/Pd loading, which was taken advantage of by Fukai and Okuma [51] to create a new phase with superabundant vacancies which we can write as $Pd_{0.75}H$. That this phase is thermodynamically favored at high loading suggests that we ought to at least be aware of the phase in connection with our discussion of D/Pd ratios in excess of unity. For example, in equilibrium we would expect the vacancy phase have a big impact on the phase diagram in this case; however, near room temperature vacancy diffusion is extremely slow so that one would not expect the vacancy phase to form through this mechanism over the course of an experiment. Nevertheless, one could imagine that if the D/Pd loading were sufficiently high then sufficient energy could be present to drive a phase change much more rapidly; as yet we are not aware of experimental evidence for this.

These arguments ultimately lead us back to a picture in which tetrahedral site occupation must be contemplated then when the D/Pd loading is sufficiently high. Within this picture a new set of issues arise. The first concerns how large the excitation energy is for O-site to T-site excitation. For example, if the excitation energy is large, then we would expect to see little T-site occupation for D/Pd < 1, and then a large increment in pressure would be required to push the D/Pd loading above unity. On the other hand, if the excitation energy is more modest, then we might expect to see some tetrahedral occupation in the accessible D/Pd < 1 regime, and the regime with a D/Pd loading greater than unity should be accessible in high pressure experiments and also in electrochemical experiments.

In what follows, our focus is on the development of an empirical model for PdD at high loading. Unfortunately, there is probably not sufficient relevant data available from experiment in order to specify such a model to the degree that we might be satisfied with. However, if we broaden our perspective to include the simultaneous development of a similar model for PdH, then the situation improves significantly, given certain assumptions as to how different the model for PdD should be from the model for PdH.

2. Simple Empirical Model for O-site and T-site Occupation

In order to connect with experiment in the case of highly loaded PdD we need to construct a statistical mechanics model for O-site and T-site occupation, with site energies which depend on the D/Pd loading. We also need to account for statistical factors associated with the electronic spin, nuclear spin, and excited state degeneracy of the interstitial atoms in the O-sites and T-sites. Our first order of business then is to assemble a set of basic relations between the deuterium chemical potential and the occupation of octahedral and tetrahedral sites.

The development of the basic thermodynamic relations is straightforward; but the specification of empirical models for how the site energies depend on the D/Pd loading is not. One might argue that it should be possible to take advantage of theory in order to understand how the site energies depend on the D/Pd loading. As we will see, the precision required to obtain a useful empirical model is beyond the current state of the art. Consequently, we will need to turn to experiment in order to develop model parameters. Fortunately we have available some measurements which are helpful; these will be considered in subsequent sections, along with the fitting of model parameters to the data.

2.1. Model partition function

The starting point for the thermodynamics model is a canonical partition function which roughly follows the approach of Lacher [36] given by

$$Q = \sum_{M_T} \sum_{M_O} \frac{(N_O + N_T)!}{M_O!(N_O - M_O)!M_T!(N_T - M_T)!} z_O^{M_O} z_T^{M_T} e^{-(M_O E_O + M_T E_T)/k_B T}, \tag{1}$$

where z_O and z_T are deuterium atom partition functions associated with O-site and T-site occupation. This approach is discussed by Orondo [55]; we have generalized it to include an appropriate multinomial coefficient for the partition of deuterium atoms into O-sites and T-sites. In this formula N_O and N_T are the number of O-sites and T-sites available, and M_O and M_T are the number of deuterium atoms in O-sites and T-sites.

The partition functions for the O-site and T-site are taken to be [52]

$$\begin{aligned} \text{PdH}: \quad & z_O = z_T = 2 \times 2 \left[\sum_n \exp\left\{ -\frac{E_n}{k_B T} \right\} \right]^3, \\ \text{PdD}: \quad & z_O = z_T = 2 \times 3 \left[\sum_n \exp\left\{ -\frac{E_n}{k_B T} \right\} \right]^3 \end{aligned} \tag{2}$$

with

$$E_n = \hbar \omega_{O,T} n^s \tag{3}$$

and

$$\begin{aligned} \text{PdH}: \quad & \hbar\omega_O = 69.0 \text{ meV}, \quad s_O = 1.2, \\ \text{PdH}: \quad & \hbar\omega_T = 53.8 \text{ meV}, \quad s_T = 1.2, \\ \text{PdD}: \quad & \hbar\omega_O = 46.5 \text{ meV}, \quad s_O = 1.2, \\ \text{PdH}: \quad & \hbar\omega_T = 39.0 \text{ meV}, \quad s_T = 1.2. \end{aligned} \tag{4}$$

The O-site partition function was developed from fits to results from inelastic neutron scattering [53]. The T-site partition function was selected to have the same s_T value, and was otherwise optimized fit in the analysis of solubility data for α-phase PdH_x and PdD_x [52].

In the D_2 chemical potential model that we make use of as in reference [54], we presumed a singlet electronic ground state with statistical weight 1 for the molecule; in a simple picture for atomic deuterium in the lattice the electronic spin degeneracy could reasonably be taken to be 2. For the molecule, we included the nuclear spin degeneracy which was reduced by the generalized Pauli principle; now we can keep track of the full nuclear spin degeneracy of the spin 1 deuterons. Analogous arguments apply in the case of PdH. The site energies E_O and E_T are assumed to vary with loading, with the temperature constant at 300 K in this study.

2.2. Deuterium chemical potential in the solid phase

For the chemical potential of O-site deuterium atoms we can write

$$-\frac{\mu_{\rm O}}{k_{\rm B}T} = \frac{\partial}{\partial M_{\rm O}} \ln\left\{ \frac{(N_{\rm O}+N_{\rm T})!}{M_{\rm O}!(N_{\rm O}-M_{\rm O})!M_{\rm T}!(N_{\rm T}-M_{\rm T})!} z_{\rm O}^{M_{\rm O}} z_{\rm T}^{M_{\rm T}} {\rm e}^{-(M_{\rm O}E_{\rm O}+M_{\rm T}E_{\rm T})/k_{\rm B}T} \right\}. \tag{5}$$

A similar expression occurs now for the T-site deuterium atoms

$$-\frac{\mu_{\rm T}}{k_{\rm B}T} = \frac{\partial}{\partial M_{\rm T}} \ln\left\{ \frac{(N_{\rm O}+N_{\rm T})!}{M_{\rm O}!(N_{\rm O}-M_{\rm O})!M_{\rm T}!(N_{\rm T}-M_{\rm T})!} z_{\rm O}^{M_{\rm O}} z_{\rm T}^{M_{\rm T}} {\rm e}^{-(M_{\rm O}E_{\rm O}+M_{\rm T}E_{\rm T})/k_{\rm B}T} \right\}. \tag{6}$$

The partial derivatives can be evaluated approximately in the limit that a macroscopic number of sites and deuterium atoms is involved to yield [55]

$$\begin{aligned}\mu_{\rm O} &= E_{\rm O} + M_{\rm O}\frac{\partial}{\partial M_{\rm O}}E_{\rm O} + M_{\rm T}\frac{\partial}{\partial M_{\rm O}}E_{\rm T} - k_{\rm B}T\ln\frac{N_{\rm O}-M_{\rm O}}{M_{\rm O}} - k_{\rm B}T\ln z_{\rm O} \\ &= E_{\rm O} + \theta_O\frac{\partial}{\partial \theta_O}E_{\rm O} + \theta_{\rm T}\frac{\partial}{\partial \theta_O}E_{\rm T} - k_{\rm B}T\ln\frac{1-\theta_O}{\theta_O} - k_{\rm B}T\ln z_{\rm O},\end{aligned} \tag{7}$$

$$\begin{aligned}\mu_{\rm T} &= E_{\rm T} + M_{\rm T}\frac{\partial}{\partial M_{\rm T}}E_{\rm T} + M_{\rm O}\frac{\partial}{\partial M_{\rm T}}E_{\rm O} - k_{\rm B}T\ln\frac{N_{\rm T}-M_{\rm T}}{M_{\rm T}} - k_{\rm B}T\ln z_{\rm T} \\ &= E_{\rm T} + \theta_{\rm T}\frac{\partial}{\partial \theta_{\rm T}}E_{\rm T} + \theta_O\frac{\partial}{\partial \theta_{\rm T}}E_{\rm O} - k_{\rm B}T\ln\frac{2-\theta_{\rm T}}{\theta_{\rm T}} - k_{\rm B}T\ln z_{\rm T}.\end{aligned} \tag{8}$$

In these formulas $E_{\rm O}$ and $E_{\rm T}$ depend on the O-site and T-site loading, as well as on the temperature. The O-site and T-site occupation fractions are referenced to the number of Pd atoms in the absence of vacancies, which is the same as the number of O-sites

$$\theta_{\rm O} = \frac{M_{\rm O}}{N_{\rm O}} = \frac{M_{\rm O}}{N_{\rm Pd}}, \tag{9}$$

$$\theta_{\rm T} = \frac{M_{\rm T}}{N_{\rm O}} = \frac{M_{\rm T}}{N_{\rm Pd}}. \tag{10}$$

According to these definitions the O-site fractional occupation $\theta_{\rm O}$ varies between 0 and 1, while the T-site fractional occupation $\theta_{\rm T}$ varies between 0 and 2. In equilibrium the different chemical potentials are equal

$$\mu_{\rm O} = \mu_{\rm T} = \mu_{\rm D}. \tag{11}$$

We note in connection with this discussion the approach of Ref. [56].

2.3. Reduction of the model

If the first-principles theoretical models were sufficiently good, then we could make use of the results of density functional calculations to determine how the O-site and T-site energies depend on the distribution of the atoms among the different sites, at least on average. From previous experience with such calculations, we know that the average configuration energies from Quantum Espresso calculations can be off by more than 100 meV [55,57]. While the agreement between DFT theory and experiment must be considered in this case to be excellent (given how difficult the calculation is), such a level of agreement is not useful for the modeling under consideration here.

To simplify things for the development of a useful empirical model, we will assume that the site energies depend on the total D/Pd loading (fractional interstitial occupation) θ

$$\theta = \theta_{\rm O} + \theta_{\rm T}. \tag{12}$$

The total loading θ under these definitions varies between 0 and 3. In this case, our thermodynamic relations reduce to

$$\mu_{\rm D} = E_{\rm O} + \theta_{\rm O}\frac{\partial E_{\rm O}}{\partial\theta} + \theta_{\rm T}\frac{\partial E_{\rm T}}{\partial\theta} - k_{\rm B}T\ln\frac{1-\theta_{\rm O}}{\theta_{\rm O}} - k_{\rm B}T\ln z_{\rm O}, \tag{13}$$

$$\mu_{\rm D} = E_{\rm T} + \theta_{\rm T}\frac{\partial E_{\rm T}}{\partial\theta} + \theta_{\rm O}\frac{\partial E_{\rm O}}{\partial\theta} - k_{\rm B}T\ln\frac{2-\theta_{\rm T}}{\theta_{\rm T}} - k_{\rm B}T\ln z_{\rm T}. \tag{14}$$

In writing this we presume that the site energies $E_{\rm O}$ and $E_{\rm T}$ depend on loading θ and on temperature.

2.4. Inclusion of PdV terms

The lattice expands by an incremental volume V_D when a deuterium atom enters the lattice. If the lattice is in deuterium gas, this expansion does work on the gas. We can take this effect into account by augmenting the model chemical potential with PdV terms according to

$$\mu_{\rm D} = E_{\rm O} + \theta_{\rm O}\frac{\partial E_{\rm O}}{\partial\theta} + \theta_{\rm T}\frac{\partial E_{\rm T}}{\partial\theta} - k_{\rm B}T\ln\frac{1-\theta_{\rm O}}{\theta_{\rm O}} - k_{\rm B}T\ln z_{\rm O} + PV_{\rm D}, \tag{15}$$

$$\mu_{\rm D} = E_{\rm T} + \theta_{\rm T}\frac{\partial E_{\rm T}}{\partial\theta} + \theta_{\rm O}\frac{\partial E_{\rm O}}{\partial\theta} - k_{\rm B}T\ln\frac{2-\theta_{\rm T}}{\theta_{\rm T}} - k_{\rm B}T\ln z_{\rm T} + PV_{\rm D}. \tag{16}$$

where $V_{\rm D}$ is about 2.9 Å^3 (we will adopt the save incremental volume for hydrogen). At low pressure these terms contribute very little, which is why they are usually neglected; however at high pressure in the vicinity of 1 GPa the PdV terms have a noticeable impact on the solubility.

2.5. Site energy models and temperature independence

The models above are reasonably general, and one might make use of them in connection with a sophisticated model with temperature-dependent site energies that are nonlinear in loading. We are interested in reducing the model even further (in order to reduce the number of degrees of freedom) in order to apply to restricted conditions. To this end, we consider a version for use under constant temperature conditions where the site energies are locally quadratic in the loading θ. It will be convenient to use a parameterization for the O-site energy given by

$$E_{\rm O}(\theta) = E_{\rm O}(\theta_0) + (\theta - \theta_0)E'_{\rm O}(\theta_0) + \frac{1}{2}(\theta - \theta_0)^2 E''_0(\theta_0). \tag{17}$$

We will take (somewhat arbitrarily)

$$\theta_0 = 0.60, \tag{18}$$

which is near the β-phase boundary of the miscibility gap.

We parameterize the T-site energy according to

$$E_{\rm T}(\theta) = E_{\rm O}(\theta) + \Delta E(\theta). \tag{19}$$

We see in this that the T-site energy is referenced to the O-site energy, with an O-site to T-site excitation energy specified as $\Delta E(\theta)$. In what follows we will consider a version of the model with constant excitation energy, and later on a more sophisticated version of the model with $\Delta E(\theta)$ chosen to match values inferred from experimental measurements.

2.6. Supplemental constraints

We see that there are three parameters and one function to be specified for an empirical model for loading in PdD, and three additional parameters and another function to be specified for an analogous empirical model for loading in PdH. From our perspective, the experimental data set that is available is insufficient to determine the 6 parameters and two functions required for the two models under consideration.

It is possible to reduce the number of free parameters by adding supplementary constraints on the parameters for PdD and PdH. It has been noted in the literature that the pressure as a function of loading curves for PdH and PdD in the β-phase region are offset from one another, but otherwise are very similar. We will take the liberty of presuming that this similarity extends for the O-site energy over the entire range of interest, which leads to the supplementary constraints

$$E'_{\rm O}(\theta)\Big|_{\rm PdH} = E'_{\rm O}(\theta)\Big|_{\rm PdD} \tag{20}$$

$$E''_{\rm O}(\theta)\Big|_{\rm PdH} = E''_{\rm O}(\theta)\Big|_{\rm PdD}. \tag{21}$$

For the O-site to T-site excitation energy, it would be reasonable to assume that the energy difference differs by the zero point energy

$$\Big[\Delta E(\theta)\Big]_{\rm PdH} = \Big[\Delta E(\theta)\Big]_{\rm PdD} + \Delta E_{\rm zp}. \tag{22}$$

The difference found for the α-phase does not match this requirement [52], but is not far off. In what follows we will make use of the experimental energy difference as best we know it, and use this relation as a check.

The biggest difficulty in the development of empirical models is in determining relevant constraints that can reduce the number of degrees of freedom that need to be specified. By supplementing our model with these constraints, we have reduced the number of degrees of freedom.

2.7. Chemical potential of deuterium in the gas phase

To proceed, we will need to evaluate the chemical potential; for this we write [55,58]

$$\mu_{\rm D} = \frac{1}{2}\mu_{\rm D_2} = \frac{1}{2}\mu_{\rm nonideal} - \frac{1}{2}k_{\rm B}T\ln z_{\rm rotvib} - \frac{E_{\rm d}}{2}, \tag{23}$$

where the nonideal contribution to the chemical potential is

$$\mu_{\rm nonideal} = k_{\rm B}T\ln\left[\frac{f}{k_{\rm B}T}\left(\frac{2\pi\hbar^2}{Mk_{\rm B}T}\right)^{3/2}\right]. \tag{24}$$

For the rotational and vibrational partition function we have

$$\mathrm{H_2}\text{:}\quad z_{\rm rotvib} = 1\sum_{\text{even } l}\sum_{n}(2l+1)\,{\rm e}^{-E_{nl}/k_{\rm B}T} + 3\sum_{\text{odd } l}\sum_{n}(2l+1)\,{\rm e}^{-E_{nl}/k_{\rm B}T}, \tag{25}$$

$$\mathrm{D_2}\text{:}\quad z_{\rm rotvib} = 6\sum_{\text{even } l}\sum_{n}(2l+1)\,{\rm e}^{-E_{nl}/k_{\rm B}T} + 3\sum_{\text{odd } l}\sum_{n}(2l+1)\,{\rm e}^{-E_{nl}/k_{\rm B}T}. \tag{26}$$

We made use of the fits of Urey and Rittenberg [59] for the rotational and vibrational energy levels. We note that the nuclear spin degrees of freedom are included explicitly in these relations [54]. To model the fugacity, we have available the model of Joubert for H_2 [60], and the model of Joubert and Thiebaut [61] for D_2. We have chosen in this case to use the H_2 model of Joubert [60] in both cases, in light of the discussion in Ref. [62]. The deuterium chemical potential that results in the case of PdD is shown in Fig. 2.

2.8. Matching with experiment at modest pressure

The pressure as a function of loading has been studied for both PdD and PdH in gas loading experiments at modest D_2 and H_2 pressure, and the resulting $P-C-T$ curves are reasonably well known [64]. These pressure versus loading curves are reasonably well fit by the empirical solubility relations given by Baranowski et al. [42]

$$\ln f_{\rm H_2} = -\frac{(100.4-90.1\theta)\ (\text{kJ mol}^{-1})}{RT} + \frac{106.4\ (\text{J mol}^{-1}\text{K}^{-1})}{R} + 2\ln\frac{\theta}{1-\theta}, \tag{27}$$

$$\ln f_{\rm D_2} = -\frac{(95.6-90.1\theta)\ (\text{kJ mol}^{-1})}{RT} + \frac{106.4\ (\text{J mol}^{-1}\text{K}^{-1})}{R} + 2\ln\frac{\theta}{1-\theta}. \tag{28}$$

The resulting pressure versus loading curves are shown in Fig. 3. One can see that the two curves are parallel with an offset.

If we presume no T-site occupation, and that the O-site energy is linear in the total loading θ, then we can obtain estimates for four of the empirical model parameters

$$\text{PdH}:\quad E_{\rm O}(\theta_0) - k_{\rm B}T\ln z_{\rm O} + \frac{E_{\rm D}}{2} = -391.8\ \text{meV},\quad E'_{\rm O}(\theta_0) = 233.5\ \text{meV}, \tag{29}$$

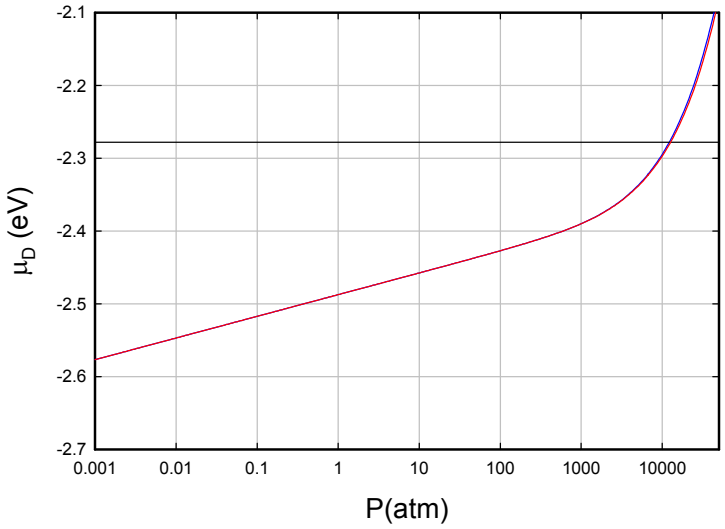

Figure 2. Deuterium chemical potential at 300 K as a function of pressure; with the D_2 fugacity from [59] (red line); with the H_2 fugacity from [60] (blue line); and half the dissociation energy $-E_d/2$ (black line).

$$\text{PdD}: \quad E_O(\theta_0) - k_B T \ln z_O + \frac{E_D}{2} = -399.1 \text{ meV}, \quad E'_O(\theta_0) = 233.5 \text{ meV}. \tag{30}$$

The slope parameters are the same here due to the construction of the empirical fits of Baranowski et al. [42] above. We used for the dissociation energy of H_2 2×2.23899 eV, and for the dissociation energy of D_2 2×2.27806 eV.

We can estimate the contribution of the $k_B T \ln z_O$ factors using a 3D SHO model to be

$$\text{PdH}: \quad k_B T \ln z_O = 41.4 \text{ meV}, \tag{31}$$

$$\text{PdD}: \quad k_B T \ln z_O = 60.4 \text{ meV}. \tag{32}$$

The corresponding estimates for $E_O(\theta_0)$ are

$$\text{PdH}: \quad E_O(\theta_0) + \frac{E_D}{2} = -350.4 \text{ meV} \quad \text{(SHO)}, \tag{33}$$

$$\text{PdD}: \quad E_O(\theta_0) + \frac{E_D}{2} = -338.8 \text{ meV} \quad \text{(SHO)}. \tag{34}$$

If we make use of the non-SHO partition functions given above (from Ref. [52]) we obtain

$$\text{PdH}: \quad E_O(\theta_0) + \frac{E_D}{2} = -350.6 \text{ meV} \quad \text{(non} - \text{SHO)}, \tag{35}$$

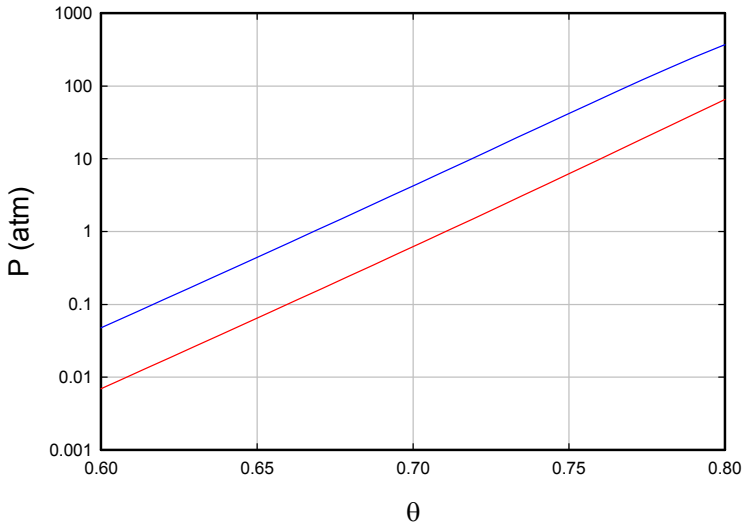

Figure 3. Equilibrium pressure at 300 K as a function of loading based on the parameterization of Baranowski et al. [42] for PdH (red line) and PdD (blue line).

$$\text{PdD}: \quad E_{\rm O}(\theta_0) + \frac{E_{\rm D}}{2} = -339.8 \text{ meV} \quad (\text{non} - \text{SHO}). \tag{36}$$

We might have expected to see a difference between PdH and PdD due to the zero-point energy contribution (which is estimated to be 31 meV by Ke and Kramer [63]); however the results here are much closer.

2.9. Fitting PdH at higher pressure

We would like to extend this general approach to higher loading if possible; unfortunately we lack systematic pressure versus loading data at higher pressure. There are some high pressure measurements of PdH that were reported by Tkacz and Baranowski [65] that look to be useful in the context of the present analysis. In this work data points are reported at H/Pd loadings between 0.90 and 0.995. Since our focus at the moment is on the O-site energy, we propose here to make use of the two data points with the lowest values of θ, as these have the best chance of being relatively free of tetrahedral occupation. It is possible to arrange for a weighted least squares fit based on

$$\mu_{\rm H} = E_{\rm O} + \theta_{\rm O}\frac{\partial E_{\rm O}}{\partial \theta} - k_{\rm B}T \ln \frac{1-\theta_{\rm O}}{\theta_{\rm O}} - k_{\rm B}T \ln z_{\rm O} + PV_{\rm H} \tag{37}$$

with results shown in Fig. 4. We see that the pressure versus loading curve that results looks very plausible. In this case the fitting parameters are

$$\text{PdH}: \quad E_{\rm O}(\theta_0) + \frac{E_{\rm D}}{2} = -385.8 \text{ meV}, \quad E'_{\rm O}(\theta_0) = 291.8 \text{ meV}, \quad E''_{\rm O}(\theta_0) = -150.3 \text{ meV}. \tag{38}$$

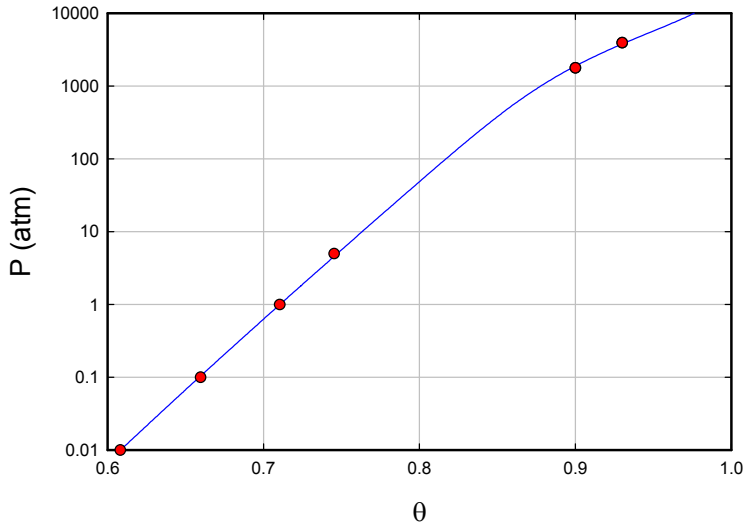

Figure 4. Least squares fit to selected pressure as a function of loading points for PdH at 300 K as a function of loading; points used for the fit (red circles); weighted least squares fit (blue line).

According to the supplemental constraints, we propose to develop an equivalent O-site energy model for PdD by shifting the O-site energy for PdH by a constant to match the pressure at the β-phase boundary; this leads to

$$\text{PdD}: \quad E_{\rm O}(\theta_0) + \frac{E_{\rm D}}{2} = -374.8 \text{ meV}, \quad E'_{\rm O}(\theta_0) = 291.8 \text{ meV}, \quad E''_{\rm O}(\theta_0) = -150.3 \text{ meV}. \tag{39}$$

2.10. Discussion

We are interested in the development of empirical models for the O-site and T-site energies in to be used in conjunction with an equilibrium statistical thermodynamics model for the O-site and T-site fractional occupation. In general one would like many degrees of freedom in an empirical model in order to develop the best match to the available experimental data sets. For our model it will not be straightforward to arrange for a unique determination of all of the parameters directly from experimental data, simply because we lack the relevant experimental measurements of PdD at high pressure, and we also lack experimental measurements of site-dependent occupancy at high loading.

The model under discussion assumes a quadratic dependence of the O-site energy on the total loading θ, and an O-site to T-site excitation energy that is to be discussed. There are six parameters and two functions to be specified for PdH and PdD. To reduce the number of free parameters we introduce supplementary constraints, which insures that the resulting models will differ only by offset energies. This allows us to make use of the high pressure measurements in PdH to estimate what happens in PdD at high pressure, below the point where T-site occupation becomes important. At this point we have initial estimates for the six parameters needed for our empirical models.

3. Input on T-site Occupation

At present there is no unambiguous direct experimental observation of bulk tetrahedral site occupation in equilibrium at high loading in PdH or PdD. Consequently, it has not been established conclusively what phase might be present in PdH or PdD above a loading of unity; only a few authors even claim to have observed PdH or PdD above a loading of unity. Nevertheless, we will proceed in what follows under the presumption that at high loading interstitial hydrogen or deuterium in equilibrium occupies tetrahedral sites.

The big issue in modeling T-site occupation is in determining the O-site to T-site excitation energy. This excitation energy has as yet not been determined experimentally. There are a number of theoretical calculations in the literature; however, there is a reasonably wide range of excitation energies predicted, and no reason to believe that the calculations are sufficiently accurate to be able to predict T-site occupation usefully. There is some neutron diffraction data which looks interesting at lower loading, which we consider in this section. The O-site to T-site excitation energy near a loading of unity will remain undetermined until the next section.

3.1. O-site to T-site excitation energy calculations

About 25–30 years ago, one could find literature values for the excitation energy near 300 meV [39,41]. Subsequently the problem has been addressed with embedded atom models, density functional calculations, and quantum chemistry calculations. A sizeable spread in the calculated O-site to T-site excitation energy is found, as shown in Table 1.

Based on this we might expect the O-site to T-site excitation energy near zero loading to be between about 50 and 295 meV, and that it probably increases with increasing loading.

3.2. Quasi-elastic neutron diffraction experiments

Tetrahedral occupation can be observed in quasi-elastic neutron diffraction experiments, which have been reported in the case of PdD. For example, if only O-sites are occupied, then the lattice structure is FCC which would be expected to give an associated FCC diffraction pattern. However, if significant tetrahedral occupation occurs, then the part of the diffraction pattern associated with the deuterons would would instead be consistent with the Fm3m space group. X-ray scattering is not useful in this application since deuterium atoms have no scattering power in the X-ray regime. The deuterium occupation can be determined then from the strength of the new neutron diffraction peaks that are not present in the FCC part of the spectrum.

Table 1. Energy difference (meV) between O-site and T-site occupation for different studies.

Reference	PdD/PdH	$\Delta E(\theta = 0)$	$\Delta E(\theta = 1)$
[39]	PdH	290	
[41]	PdD	295	350
[66]	PdH		213
[66]	PdD		150
[63]	PdD	50 ($\theta = 0.25$)	
[67]	PdH	80	
[68]	PdH	160	
[69]	PdH	160	
[70]	PdH	70	95
[55]	PdH		385
[71]	PdH	142	

An early attempt to determine tetrahedral occupation in this way was reported by Rotella et al. [72] in an electrochemical experiment near room temperature. Positive observations of diffraction lines from the Fm3m space group were reported by Pitt and Gray [73] in experiments done at 309°C, with comparable results subsequently obtained by McLennan et al. [74] in experiments done at similar temperatures. Negative results for tetrahedral occupation were found by Widenmeyer et al. [75] in experiments carried out at 177°C .

3.3. Role of monovacancies

We are confronted with a seeming contradiction where experiments which seem similar given different results. To make progress, it will be useful to have a picture in mind, and allow us to understand the model that results better.

We might begin with the measurements of Widenmeyer et al. [75] and assert somewhat arbitrarily that they argue they they tell us that there is no observable T-site occupation up to a D/Pd loading of 0.72 at a temperature of 177°C. We might take this one step further and assert that the data point that appears in Fig. 6 of Ref. [74] for a D/Pd loading of about 0.96 with a tetrahedral occupation somewhere between 0 and 2% at 25°C provides for the strictest experimental upper limit relevant for our model near stoichiometric loading.

If so, then what is the situation with the much higher levels of T-site occupation reported near 309°C in [73,74]? There are two possibilities. One is that the positive observations might be due (at least in part) to deuterium trapped in T-sites in monovacancies [76–78]. The idea is that if the sample was loaded reasonably well at elevated temperatures, then Pd vacancies become stabilized, and one might expect them to be able to form via atomic self-diffusion (vacancy diffusion) if the sample is held at elevated temperature sufficiently long [79]. We would expect deuterium to be trapped in vacancies, because the binding energy is be greater than for bulk O-site occupation. The O-site to T-site excitation energy in a monovacancy is known to be very small in the case of Ni [80], which is consistent with the relative occupation observed in Pd monovacancies [78].

Another possibility is that the observations reported by Pitt and Gray [73], and also by McLennan et al. [74], are basically correct. In this case one might argue that the O-site to T-site excitation energy is high in the β-phase, and also in the (dominant) β-phase component in the miscibility gap. If the sensitivity of the experiment of Widenmeyer et al. [75] were low, then the relatively weak signals from T-site occupation might not have been apparent.

Further experimentation will be required to resolve this issue. If we take the positive T-site observations as valid, then we end up with a model which looks to be generally consistent with what we found from an analysis of α-phase solubility data, and also what we will find shortly from high pressure experiments. If these neutron diffraction experiments are impacted by the presence of monovacancies, then our estimate for the excitation energy will be a lower bound (if diffraction from excited states contributes in equal measure to diffraction from the ground state).

3.4. Constraint on the O-site to T-site excitation energy

Given the discussion above, we propose to make use of the neutron diffraction measurements at lower temperature to provide a constraint on the O-site to T-site excitation energy at a D/Pd loading near unity. If we work with the low tetrahedral occupation observed at a D/Pd ratio of 0.96 at 25°C, we can use this to estimate an upper limit on the excitation energy at that loading and temperature.

For the analysis of a single D/Pd loading point, we can develop a local relation between the O-site to T-site excitation energy and the loading from the more general version of the model

$$\mu_D = E_O + \theta_O \frac{\partial}{d\theta} E_O + \theta_T \frac{\partial}{d\theta} E_T - k_B T \ln \frac{1-\theta_O}{\theta_O} - k_B T \ln z_O + P V_D,$$

$$\mu_{\rm D} = E_{\rm T} + \theta_{\rm T}\frac{\partial}{\partial d}E_{\rm T} + \theta_{\rm O}\frac{\partial}{d\theta}E_{\rm O} - k_{\rm B}T\ln\frac{2-\theta_{\rm T}}{\theta_{\rm T}} - k_{\rm B}T\ln z_{\rm T} + PV_{\rm D}$$

and subtract to obtain

$$E_{\rm T} - E_{\rm O} = k_{\rm B}T\left\{\ln\left(\frac{2-\theta_{\rm T}}{\theta_{\rm T}}\frac{\theta_{\rm O}}{1-\theta_{\rm O}}\right) + \ln\frac{z_{\rm T}}{z_{\rm O}}\right\}. \tag{40}$$

Results are shown in Table 2 (computed with the non-SHO partition functions). We do not know the lower limit of sensitivity in this experiment, so we have computed excitation energies for three possible low values of T-site occupation. We see that the O-site to T-site excitation energy must be greater than about 200 meV to be consistent with the low T-site occupation point in [74].

3.5. Estimate of excitation energies

In experiments of Pitt and Gray [73], and in experiments reported by McLennan et al. [74] positive observations of T-site occupation are reported. We would like to analyze the data point by point using an approach similar to the one used above. In this case we might assume either that we have deuterium occupation of T-sites, in which case we expect $E_{\rm T} - E_{\rm O}$ to be positive and large; or else we might assume that we have deuterium occupation of monovacancy traps. For this latter case, we can write

$$E_{\rm T}[V] - E_{\rm O} = k_{\rm B}T\left\{\ln\left(\frac{\Theta_{\rm V}-\theta_{\rm T}}{\theta_{\rm T}}\frac{\theta_{\rm O}}{1-\theta_{\rm O}}\right) + \ln\frac{z_{\rm T}[V]}{z_{\rm O}}\right\}, \tag{41}$$

where $\Theta_{\rm V}$ is the (unknown) fraction of monovacancy sites available.

Results are given in Table 3. One sees low but plausible O-site to T-site excitation energies under the assumption that the T-site occupation is conventional, with an O-site to T-site excitation energy that increases with loading.

The negative O-site to T-site excitation energies estimated in a simple model assuming the number of tetrahedral vacancy sites is $\Theta_{\rm V} = 0.04$ corresponds to a binding energy near 100 meV, which is a bit less than the vacancy binding energies computed by Vekilova et al. [81]. We do not know the number of vacancies present in these experiments; however, it is clear that in each case we would be able to obtain plausible (but high) solutions for vacancy concentrations consistent with the observed tetrahedral occupancy.

3.6. O-site and T-site occupation for different excitation energies

It seems to be useful to examine model predictions for the O-site and T-site occupation as a function of the total loading for different assumed O-site to T-site excitation energies. We expect the O-site to T-site excitation energy to depend

Table 2. Lower bound on excitation energy from neutron diffraction experiment at $\theta = 0.96$ at 25°C, assuming different values for T-site occupation.

θ	$\theta_{\rm O}$	$\theta_{\rm T}$	$E_{\rm T} - E_{\rm O}$ (meV)
0.96	0.955	0.005	224.6
0.96	0.950	0.01	203.9
0.96	0.960	0.02	181.0

Table 3. O-site to T-site excitation energies estimated from the neutron diffraction data of Pitt and Gray [73]. The $E_T - E_O$ number are for conventional T-site occupation [Equation (40)]; and the $E_T[V] - E_O$ numbers are for T-sites in monovacancies Eq. (41). The number of vacancy sites for this model is assumed to be $\Theta_V = 0.04$.

θ_O	θ_T	$E_T - E_O$ (meV)	$E_T[V] - E_O$ (meV)
0.068	0.016	133	-115
0.118	0.018	158	-96
0.161	0.021	168	-93
0.231	0.022	188	-76
0.355	0.030	203	-96
0.384	0.033	204	-118

on the D/Pd loading ratio, but since at present no reliable information is available with which to model, it will be convenient instead to present curves at constant excitation energies. We make use of the local isotherm for O-site and T-site occupation at constant loading [55]

$$\left(\frac{1-\theta_O}{\theta_O}\right)\left(\frac{\theta_T}{2-\theta_T}\right) = \frac{z_T}{z_O}\exp\left\{-\frac{(E_T - E_O)}{k_B T}\right\}. \tag{42}$$

Results are shown in Fig. 5. From this one can get some intuition as to how abrupt the transition from O-site occupation to T-site occupation is. For example, if the excitation energy were 500 meV, there would be an abrupt change in the

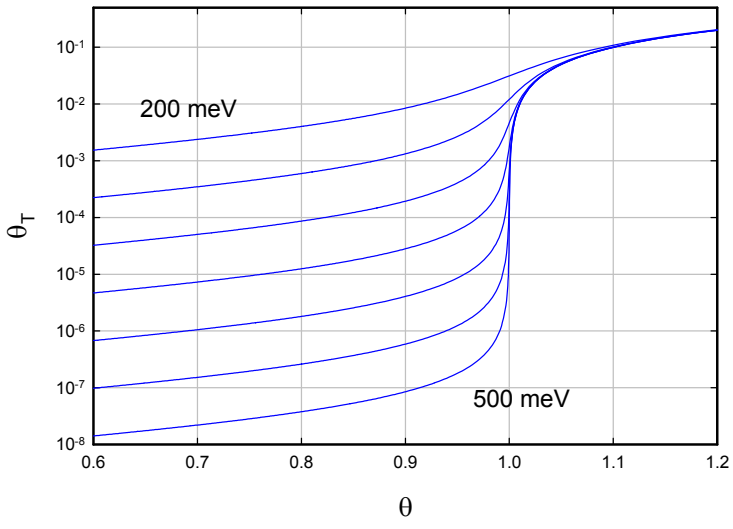

Figure 5. Tetrahedral fraction θ_T as a function total D/Pd loading θ for O-site to T-site energies of 200, 250, 300, . . ., 500 meV.

T-site occupation and a corresponding substantial change in the chemical potential which could in principle be detected in electrochemical measurements.

3.7. Discussion

It seems clear that we could learn much from neutron diffraction experiments carried out on PdD samples that are highly loaded. It is possible that the neutron diffraction experiments of Pitt and Gray [73] can be interpreted as demonstrating T-site occupation in the bulk, from which low O-site to T-site excitation energies can be inferred. It is also possible that the measurements were compromised due to the presence of a large number of monovacancies, since in a monovacancy both O-sites and T-sites can be occupied with a very small difference between the site energies. Later on we will make use of the results of these measurements interpreted as referring to bulk T-site occupation to develop an empirical fit for the excitation energy as a function of loading.

4. O-site to T-site Excitation Energy at High Loading

To complete our empirical model we require estimates for the O-site to T-site excitation energy. From the discussion of the last section, we know that the O-site to T-site excitation energy in PdD near unity loading must be greater than about 200 meV. Our goal in this section is to attempt to develop estimates for the excitation energy near unity for both PdD and PdH by comparing model predictions with experimental data at high pressure.

4.1. PdH at high loading

Let us return now to the high pressure PdH experiments of Tkacz and Baranowski [65], and compare results from the model with measured data points. By trying different values for the constant excitation energy, we find that the minimum error occurs for an excitation energy of 225.6 meV. The model parameters in this case are

$$\text{PdH}: \quad E_{\rm O}(\theta_0) + \frac{E_{\rm D}}{2} = -408.6 \text{ meV}, \quad E'_{\rm O}(\theta_0) = 322.5 \text{ meV}, \quad E''_{\rm O}(\theta_0) = -205.1 \text{ meV}. \tag{43}$$

The resulting fit is shown in Fig. 6.

4.2. Resistance ratio standard for PdH

A table that gives estimates for the H/Pd loading in PdH corresponding to different values of the resistance ratio R/R_0 appears in Crouch-Baker et al. [21]. In this table an H/Pd loading of 1.0 corresponds to a resistance ratio of 1.067. Baranowski et al. [42] show a resistance ratio corresponding to this value at a pressure of about 1.17 GPa. The pressure at an H/Pd loading of 1.0 in the model just above is 1.23 GPa, which is close.

If we carry out a least squares fitting of the pressure versus loading data set with fixed O-site to T-site excitation energy, including the two lowest points from Tkacz and Baranwoski along with the a loading of unity at 1.17GPa, then we end up with a low O-site to T-site excitation energy of about 202 meV.

4.3. Resistance ratio standard for PdD

One resistance ratio calibration curve currently in use for PdD (see [5]) gives a D/Pd loading of unity at a resistance ratio R/R_0 of 1.25, which corresponds to a D_2 equilibrium pressure of 1.94 GPa. A consistent model with constant O-site to T-site excitation energy is optimized with an excitation energy of 237 meV.

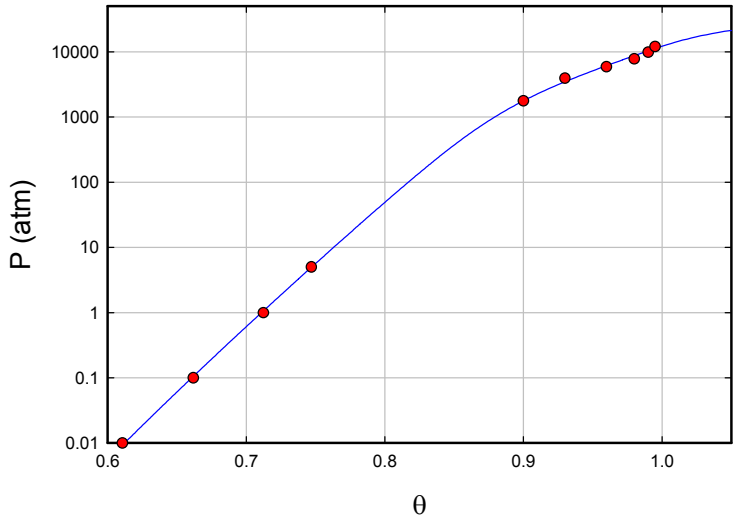

Figure 6. Least squares fit assuming an O-site to T-site excitation energy of 225.6 meV (independent of loading) to selected pressure as a function of loading points for PdH at 300 K as a function of loading; points used for the fit (red circles); least squares fit (blue line).

4.4. Resistance ratio versus fugacity for PdD at high loading

High pressure experiments with PdD were reported by Baranowski et al. [42] in which the applied D_2 reached as high as 3.1 GPa. Unfortunately the loading was not measured in these experiments, so we do not have a data set that we can compare directly with the model. However, it was noted in this paper that a noticeable break in the resistance ratio occurred at $\log_{10} f$ was about 9.3 (with fugacity assumed to be in atmospheres), which corresponds to a pressure of about 2 GPa.

We have used the model to compute θ as a function of the fugacity in order to see what O-site to T-site excitation energy might be relevant. Model results in the case of constant O-site to T-site excitation energy are shown in Fig. 7. We see that we can arrange for an intercept near $\log_{10} f = 9.3$ for an excitation energy of about 225 meV.

It may be that the determination of the resistance ratio curve involved an interpretation of the change of slope of the resistance ratio curve versus $\log_{10} f$ as defining where a D/Pd loading of unity occurs. In principle the argument here is basically the same, except that the model under discussion results in a shift in pressure. If we assume that the change in slope of the deuterium occupation fraction as a function of $\log_{10} f$ is correlated to the change in the slope of the resistance ratio as a function of $\log_{10} f$, then we conclude that $\theta = 1$ occurs closer to a pressure of 1.87 GPa at a resistance ratio R/R_0 near 1.28.

4.5. Zero-point energy considerations

We often think of PdH and PdD as being very similar other than due to differences attributable to the zero-point energy. Consequently, we might expect the O-site to T-site excitation energy in PdH to be larger than the excitation energy in PdD by the zero-point energy difference. For this discussion, we make use of the calculations of Ke and Kramer [63] for which the difference in zero-point energies for the O-site is

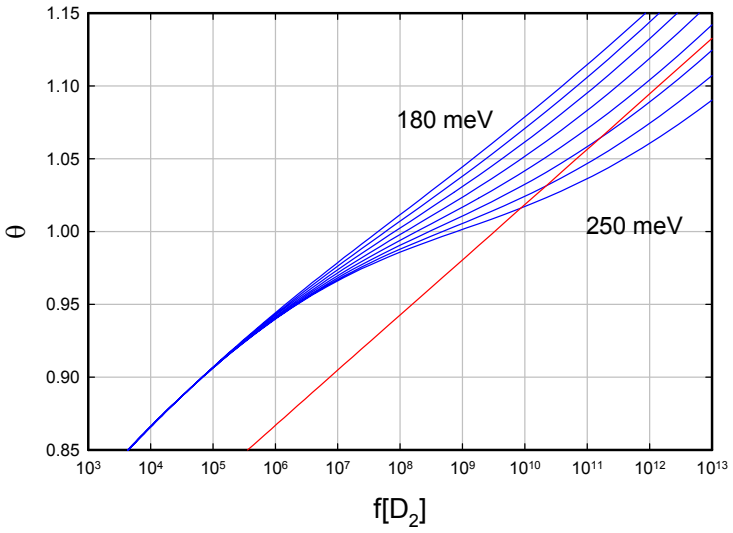

Figure 7. D/Pd ratio θ as a function of fugacity for simple models with constant O-site to T-site energies of 180, 190, . . ., 250 meV (blue lines); line with matched slope and intercept at $\log_{10} f = 9.3$(red).

$$\Delta E_{\rm O}(\text{H-D}) = 98.4 - 67.4 = 31.0 \text{ meV}. \tag{44}$$

The corresponding difference in the zero-point energies for the T-site is

$$\Delta E_{\rm T}(\text{H-D}) = 180.6 - 128.4 = 52.2 \text{ meV}. \tag{45}$$

From this we would conclude that the O-site to T-site excitation energy in PdH should be larger than in PdD by 21.2 meV near $\theta = 0$. We note that in the analysis of α-phase solubility data in [52] we obtained a smaller difference (about 1 meV). From the analysis in this section we would conclude that the O-site to T-site excitation energies are practically the same for PdH and PdD.

At high loading near $\theta = 1$ we might expect that the lattice expansion would result in a lower local zero-point energy. However, in this case the notion of a local zero-point energy is problematic as we would expect fully developed phonon dispersion relations; in this case the zero-point energy would need to be computed by summing over all of the vibrational modes. The lattice expansion is greater for PdH than for PdD, so there is the possibility that the zero-point contribution is reduced for PdH relative to PdD.

4.6. X-ray and R/R_0 data of Knies et al.

Electrochemical experiments with PdD and PdH were reported by Knies et al. [29] in which high loadings were achieved, where the (bulk) resistance ratio was measured, and where the (surface) lattice constant was measured. In principle this kind of measurement would be extremely useful in sorting out solubility issues at very high loading, and

providing data with which to compare against modeling. Probably it is useful here to consider the experiment in light of the discussion above in this Section.

For the PdD B2 experiment, the resistance ratio of 1.61 was obtained, interpreted as a bulk loading of 0.95; and a surface lattice constant of 4.09 Å was measured, and interpreted as a surface loading of 0.977. If we take a resistance ratio as corresponding to an equilibrium pressure of about 0.81 GPa, then the model with constant excitation energy would give a bulk loading of 0.939, compatible with the interpretation of Knies et al.

To determine a D/Pd loading consistent with a lattice constant of 4.09 Å it would be useful to have appropriate calibration data available. For example, Schirber and Morosin [82] have reported a systematic set of measurements at 77 K, showing that the lattice constant is very nearly linear in the loading. No equivalent study has been reported near room temperature. If we developed similar linear calibrations based on Yamamoto et al. [26], or perhaps on Felici et al. [27], we would probably conclude that the surface loading was lower than 0.977. On the other hand, a systematic study in the case of PdH_x was reported by Balbaa et al. [83], and based on these measurements we would probably conclude that a lattice constant of 4.09 Å corresponds to a D/Pd loading near unity. One conclusion that we might draw from this is that it would be very useful if a systematic calibration of D/Pd loading versus lattice constant could be established at room temperature.

For PdH, a resistance ratio as low as 1.28 appears at the largest lattice constants. The associated equilibrium pressure from [42] looks to be about about 0.67 GPa. This corresponds to a loading in a model with constant excitation energy of about 0.959, which is compantible with the 0.97 interpreted reported by Knies et al. [29].

4.7. Discussion

In this section we have taken the O-site to T-site excitation energy to be constant with loading θ, which allows us to develop estimates independently for PdH and for PdD. From the high pressure loading data of Tkacz and Baranowski we infer an excitation energy of 225.6 meV; from the resistance ratio as a function of fugacity data of Ref. [42] we estimate an excitation energy of 225 meV. We might have expected the PdH excitation energy might be larger than the PdD excitation energy based on estimates for the zero-point energy. However, the analysis of this section leads to the conclusion that the two excitation energies are essentially the same, analogous to what was found in our analysis of the α-phase solubility; this is a result which in retrospect seems very plausible.

Altogether this leads to a matched set of models for PdH and PdD which we can summarize through the model parameters

$$\text{PdH}: \quad E_{\rm O}(\theta_0) + \frac{E_{\rm D}}{2} = -384.5 \text{ meV}, \quad E'_{\rm O}(\theta_0) = 289.3 \text{ meV},$$

$$E''_{\rm O}(\theta_0) = -139.6 \text{ meV}, \quad \Delta E = 225.6 \text{ meV}, \tag{46}$$

$$\text{PdD}: \quad E_{\rm O}(\theta_0) + \frac{E_{\rm D}}{2} = -373.3 \text{ meV}, \quad E'_{\rm O}(\theta_0) = 289.3 \text{ meV},$$

$$E''_{\rm O}(\theta_0) = -139.6 \text{ meV}, \quad \Delta E = 225 \text{ meV}. \tag{47}$$

Results for pressure as a function of loading θ are shown in Fig. 8. We note that the O-site energies from this model are significantly lower than the incremental enthalpy ΔH one can find in the literature, which is about 240 meV [84]. This can be understood from the differential relation between the chemical potential and the O-site and T-site energies; here

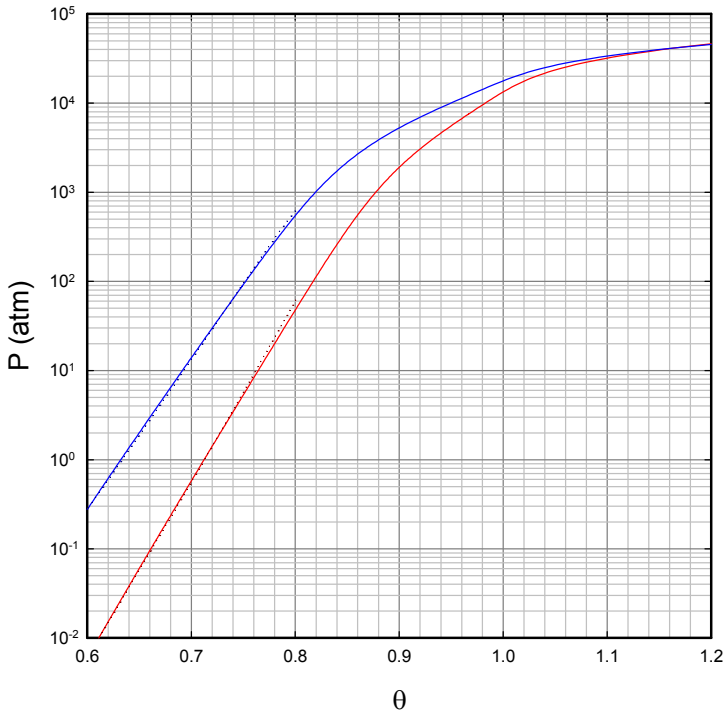

Figure 8. Model pressure as a function of loading θ at 300 K; PdH (red line); low pressure empirical model of Baranowski et al. [42] for PdH (dark red dotted line); PdD (blue line); low pressure empirical model of Baranowski et al. [42] for PdD (dark blue dotted line).

we have used a boundary condition at $\theta = 0.6$ instead of a boundary condition at $\theta = 0$. Hence the solutions for the O-site and T-site energies can be different (due to the different boundary conditions) for the same chemical potential.

In principle the established resistance ratio calibrations from the literature can be used to provide estimates for the O-site to T-site excitation energies assuming a constant excitation energy. The energies estimated in this way are 202 meV for PdH and 237 meV for PdD. Since we are expecting the excitation energies for the two cases to be close, this suggests that the different calibrations are not consistent. The resulting excitation energy estimates are nevertheless helpful in this case, as they are in the same range as estimates from other measurements.

5. O-site to T-site Excitation Energy as a Function of θ

We are interested in the specification of a model for the O-site to T-site excitation energy as a function of loading at 300 K. We have data from neutron diffraction experiments which are relevant, and which we will make use of. However, there also appears discussion in the literature on the possible impact of the T-site on diffusion which is also of interest.

5.1. Diffusion coefficient anomaly and the Sicking conjecture

We consider the diffusion coefficient anomaly, where the diffusion coefficient of D in PdD at low loading is greater than the diffusion coefficient of H in PdH at low loading. For example, consider the α-phase diffusion coefficient parameterizations given in Fukai's book [35]; if we evaluate them for PdH and PdD at $T = 300$ K, we obtain

$$D_{\rm H}(300\ {\rm K}) = 3.97 \times 10^{-7}\ {\rm cm}^2/{\rm s}, \tag{48}$$

$$D_{\rm D}(300\ {\rm K}) = 5.89 \times 10^{-7}\ {\rm cm}^2/{\rm s}. \tag{49}$$

The issue here is that the diffusion coefficient for deuterium is higher than the diffusion coefficient for hydrogen, where we might expect that the diffusion coefficient for hydrogen should be larger since hydrogen is lighter.

A resolution to this anomaly has been proposed by Sicking [85,86]. The basic idea is that the zero-point energy of the tetrahedral site is larger for PdH than for PdD, so that H might not be bound at the T-site, or perhaps the T-site is bound but leaks via tunneling. In either case, the contribution of O–T–O transitions to the diffusion coefficient might be reduced in PdH relative to PdD; this is a candidate explanation for the anomaly in the diffusion coefficient. Ke and Kramer [63] have modeled diffusion taking this into account, and find a larger diffusion coefficient for deuterium than for hydrogen (the model for deuterium in this case matches experiment, although the agreement with experiment is only qualitative in the case of hydrogen).

5.2. Implication for the O-site to T-site excitation energy

Our interest in this issue comes from the implication it has for the O-site to T-site excitation energy. For example, imagine the simplest scenario in which hydrogen in the T-site in α-phase PdH is not bound, and D in α-phase PdD is bound. The experimental activation energies are given by Sicking [86] to be 230 meV for α-phase PdH and 206 meV for α-phase PdD. Leisure et al. [87] give the barrier energies to be 232 meV for $PdH_{0.67}$ and 219 meV for $PdD_{0.67}$. The barrier energies in the two cases in the model of Ke and Kramer [63] are 204 meV for $PdH_{0.25}$ and 185 meV for $PdD_{0.25}$ (which result in theoretical activation energies close to experiment). In this scenario then we might conclude that the O-site to T-site excitation energy at low loading in PdH is above 204 meV, and the O-site to T-site excitation energy in PdD is below 185 meV.

Of course, such an argument is too simplistic, since we would want the deuterium atom to be bound and not leak in the T-site well for PdD, so we would prefer that its energy be well below 185 meV. This would suggest that we should be satisfied if the hydrogen in PdH leaks rapidly out of the T-site well in PdH. However, in either case we see that if we accept Sicking's conjecture, it implies various constraints on the O-site to T-site excitation energies.

5.3. Quasi-elastic neutron scattering and NMR experiments

We can make some progress on this by considering experimental results on quasi-elastic neutron scattering experiments, which can give information about the diffusion mechanism. For example, based on Sicking's conjecture, we might expect not to see evidence for O–T–O transitions in PdH if the T-site either is unbound or leaks; and we might expect to see evidence for O–T–O transitions in PdD if the T-site is bound and does not leak in PdD. In an early quasi-elastic neutron scattering experiment with β-phase PdH by Beg and Ross [88] the data was interpreted as being consistent with O–T–O diffusion processes, which would argue against the Sicking conjecture. However, a subsequent quasi-elastic neutron scattering experiment reported by Nelin and Sköld [89] gave a different result; in this case more accurate

measurements could be fit to models for O–O transitions, and not by O–T–O transitions. A similar conclusion was drawn based on NMR measurements [90–92].

The experimental results for PdH then are consistent with the Sicking conjecture. What we need next are analogous measurements for the O–T–O and O–O jump mechanisms in PdD. One would imagine that it should be possible to confirm the conjecture from a quasi-elastic neutron scattering or from NMR measurements, which are sensitive to the O–T–O diffusion mechanism. Unfortunately, we have as yet not been able to find reports of such measurements; consequently we do not know from experiment whether the T-site in PdD_x participates in deuterium diffusion.

5.4. Theoretical diffusion models based on the O–T–O mechanism

Quite a few theoretical treatments of the problem of diffusion have appeared in the literature. Computations of diffusion coefficients based on an O–T–O mechanism appear widely [39,67,68,70,94]. The situation in this case is perplexing. Quasi-elastic neutron scattering and NMR experiments appear to rule out the O–T–O mechanism in PdH, yet most modern treatments of the theoretical problem are based on the O–T–O mechanism.

One exception to this is an important recent paper by Yoshinari [95]. In this work a three-dimensional potential was developed from density functional calculations based on the VASP code, and numerical solutions for the eigenfunctions were obtained. Differences between diffusion in PdH and PdD in this calculation are attributed to the details of the excited state structure. The T-site ground state energy for H in Pd in this model is 240.9 meV, leading to an excitation energy of 156.2 meV.

5.5. O-site to T-site excitation energy for different θ

There does not seem to be an unambiguous conclusion from theoretical and experimental results on diffusion so far. The accuracy of the theoretical calculations is impressive, but not yet at the level we are interested in. The experimental results so far do not shed light on the excitation energy, except perhaps in providing an upper limit.

In the discussion above we were able to obtain estimates for the O-site to T-site excitation energy at different D/Pd loadings from the neutron diffraction experiments of Pitt and Gray [73]. Now that we have an estimate for the excitation energy at $\theta = 1$ from the high pressure experiments of Baranowski et al. [42], it seems reasonable to ask whether the different excitation energies might be consistent. The different results are shown together in Fig. 9, along with an empirical fit given by

$$\Delta E(\theta) = \frac{\alpha_0 + \alpha_1\theta}{1 + \beta_1\theta} \tag{50}$$

with

$$\alpha_0 = 100.676 \text{ meV}, \quad \alpha_1 = 824.259 \text{ meV},$$

$$\beta_1 = 3.1108. \tag{51}$$

Our conclusion from this discussion is that there appears to be consistency between the O-site to T-site excitation energies from the different sources. Although arising from completely different experiments, the excitation energies from the neutron diffraction data and from the high pressure data seem compatible. This would also be the case if the values from the neutron diffraction experiment were under-estimated by 10–20 meV due to interference from monovacancy occupation. The excitation energy from the analysis of the α-phase region was fine tuned to agree with

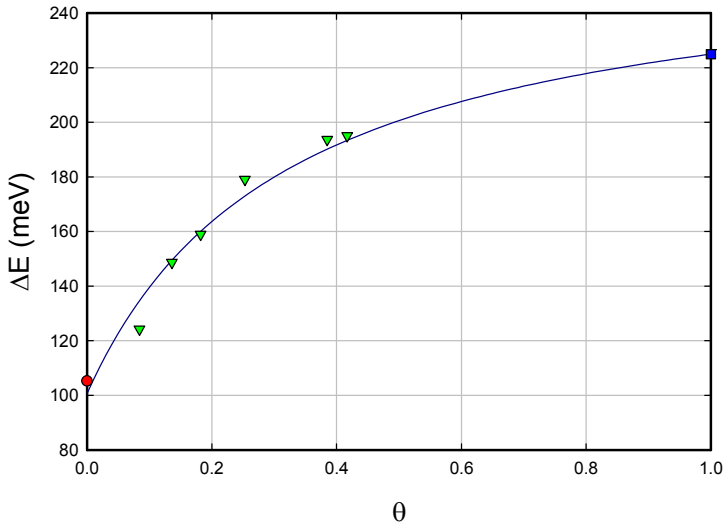

Figure 9. O-site to T-site excitation energy as a function of loading; inferred from data of Pitt and Gray [73] (green triangles); estimated from high pressure loading data of Baranowski et al. [42] (blue square); excitation energy from α-phase PdD_x analysis of Hagelstein (2015) (red circle); empirical fit (dark blue line).

the neutron diffraction data; however, had this not been done we would have ended up with an excitation energy not very different which would be compatible as an independent measurement.

In the case of PdH the excitation energy at $\theta = 0$ was estimated to be 106.5 meV at $\theta = 0$ [[52]], and 226 meV at $\theta = 1$. In both cases the excitation energy is larger by about 1 meV; so we have taken $\Delta E(\theta)$ to be larger by 1 meV in this case.

5.6. Site energy models with θ-dependent excitation energy

It is possible to optimize the O-site energy model for PdH as before, but now with the θ-dependent excitation energy model discussed above. A good fit is obtained with the parameters

$$\text{PdH}: \quad E_{\rm O}(\theta_0) + \frac{E_{\rm D}}{2} = -409.2 \text{ meV}, \quad E'_{\rm O}(\theta_0) = 328.6 \text{ meV},$$

$$E''_{\rm O}(\theta_0) = -215.5 \text{ meV}. \tag{52}$$

The corresponding fit for PdD is then

$$\text{PdD}: \quad E_{\rm O}(\theta_0) + \frac{E_{\rm D}}{2} = -399.1 \text{ meV}, \quad E'_{\rm O}(\theta_0) = 328.6 \text{ meV},$$

$$E''_{\rm O}(\theta_0) = -215.5 \text{ meV}. \tag{53}$$

These empirical fitting parameters are a bit different from those found above in the case where the excitation energy is taken to be constant with loading. The associated pressure versus loading curves are shown in Fig. 10. The O-site and T-site fractions θ_O and θ_T are shown in Fig. 11.

5.7. Discussion

Although the O-site to T-site excitation energy has been much studied over many years, there is little agreement in the literature how big the excitation energy should be. There is an anomaly in the diffusion coefficient in which the value for deuterium in palladium is larger than the value for hydrogen in palladium, which has provided the motivation for the conjecture of Sicking which would have important implications for the O-site to T-site excitation energy if true. Experimental results for quasi-elastic neutron scattering and NMR appear to rule out the O–T–O mechanism in PdH, consistent with the Sicking conjecture, but also consistent with an O-site to T-site excitation energy greater than the activation energy. Since at present we lack quasi-elastic neutron scattering results and NMR results clarifying the diffusion mechanism in PdD, there is no resolution of the problem from experiment. The recent theoretical models that focus on a mechanism presumably ruled out is perplexing.

Nevertheless, there appears to be consistency in the excitation energy developed from the analysis of neutron

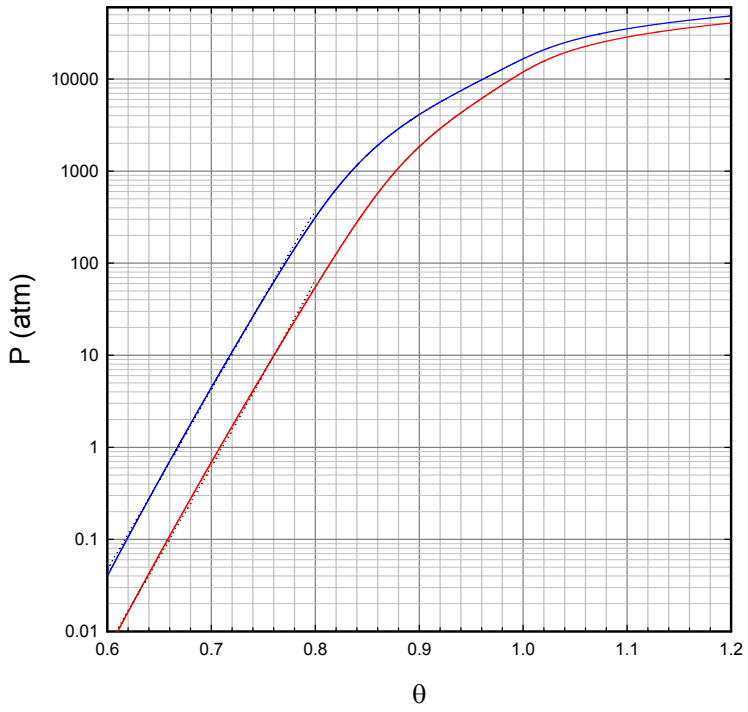

Figure 10. Model pressure as a function of loading θ at 300 K; PdH (red line); low pressure empirical model of Baranowski et al. [42] for PdH (dark red dotted line); PdD (blue line); low pressure empirical model of Baranowski et al. [42] for PdD (dark blue dotted line).

diffraction data, high pressure loading data, and from α-phase solubility data. We note that the neutron diffraction experiments are done at elevated temperature, and the high pressure measurements are done at room temperature. We took as an ansatz that the excitation energy did not vary with temperature in the analysis of the α-phase solubility data, and we were able to obtain good results. Implicit in the argument in this section is the assumption that the excitation energy is not a strong function of temperature for different loadings.

6. Possibility of new electrochemical measurements

In recent years researchers have learned how to achieve very high D/Pd loading near unity reproducibly, which constitutes an advance in electrochemistry, and potentially allows new experiments to be done which were not possible previously. We have wondered what experiments might be possible with this new capability, specifically in connection with the issues under discussion in the sections above. Here we speculate about the possibility of extending electrochemical measurements of the derivative of the chemical potential with loading, and of the Frumkin adsorption isotherm parameter, to higher loading than normally done in the hope of obtaining new information about the O-site to T-site excitation energy and solubility.

In Fig. 12 we show model results for the chemical potential as a function loading for both PdH and PdD. For many decades it has been taken as given that the hydrogen and deuterium chemical potential is linear in the loading above the miscibility gap. The chemical potential that results from the models under consideration in this paper are weakly nonlinear above the miscibility gap, and show a weak step near $\theta = 1$.

The corresponding slopes are plotted in Fig. 13. We see a weak nonlinearity in the slope above the miscibility gap from the models, and a peak near $\theta = 1$. This result is interesting, since the slope of the chemical potential is experimentally accessible. For example, we recall the measurement of the derivative of the enthalpy for PdD given in

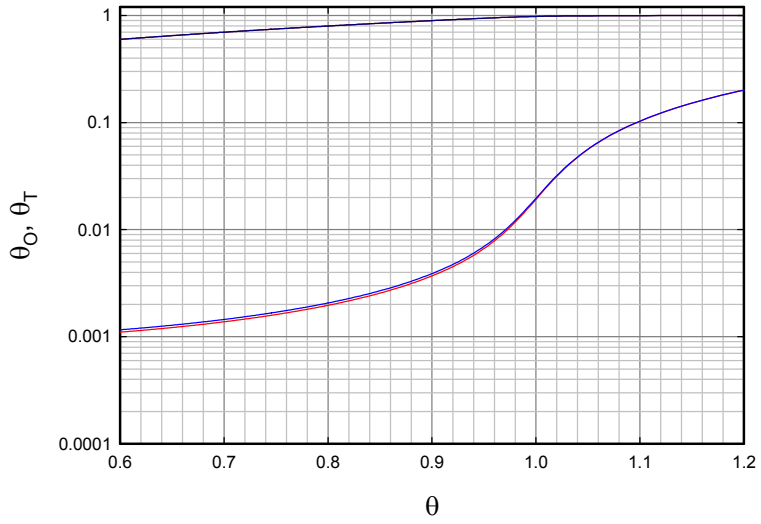

Figure 11. O-site fraction for PdH (upper dark red line, under upper dark blue line) as a function of θ; T-site fraction for PdH (lower red line); O-site fraction for PdD (upper dark blue line); T-site fraction for PdD (lower blue line).

Chun and Ra [97] which led to an estimate for the derivative of the chemical potential

$$\frac{d\mu_H}{d\theta} = 514 \text{ meV}. \tag{54}$$

The lowest value for $d\mu_D/d\theta$ in the β phase in the PdD model is 576 meV. The Frumkin adsorption isotherm parameter u is related to this derivative according to

$$u = \frac{1}{k_B T}\frac{d\mu_H}{d\theta} = 22.3. \tag{55}$$

The slope measured in [97] corresponds to $u = 19.9$.

Of interest in this discussion is that we have the possibility of learning something about the O-site to T-site excitation energy from electrochemical measurements of the slope of the chemical potential. The presence of a maximum in the slope close to $\theta = 1$ potentially gives us a way to determine where $\theta = 1$ is experimentally, and the value of the slope at the maximum places a strong constraint on the O-site to T-site excitation energy.

7. Summary and Conclusions

We have studied new empirical models for PdH and PdD for the O-site energy, and for the O-site to T-site excitation energy, in order to compare against a variety of experimental data. It must be emphasized that at this point we have no unambiguous experimental clarification that tetrahedral sites are occupied at high loading. Strictly speaking our model applies to loading to arbitrary excited state sites as long as there are two per Pd atom (and we would obtain very similar results if there were a different number of such excited state sites per Pd atom).

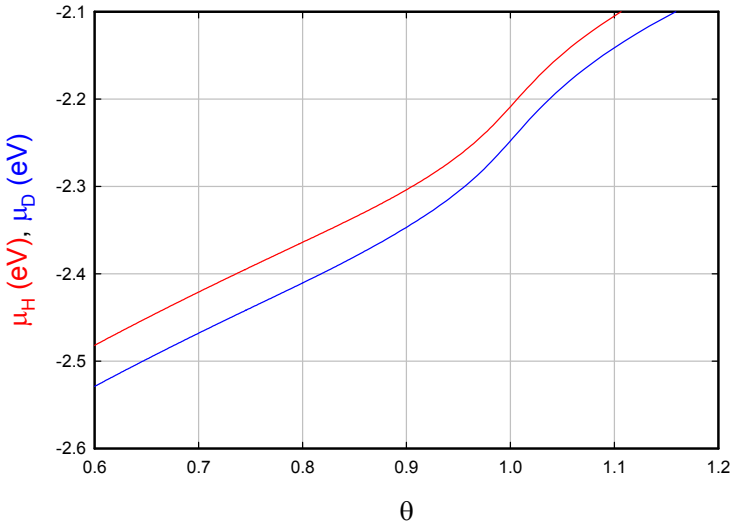

Figure 12. Model chemical potentials for PdH and PdD as a function of loading θ at 300 K with θ-dependent excitation energy.

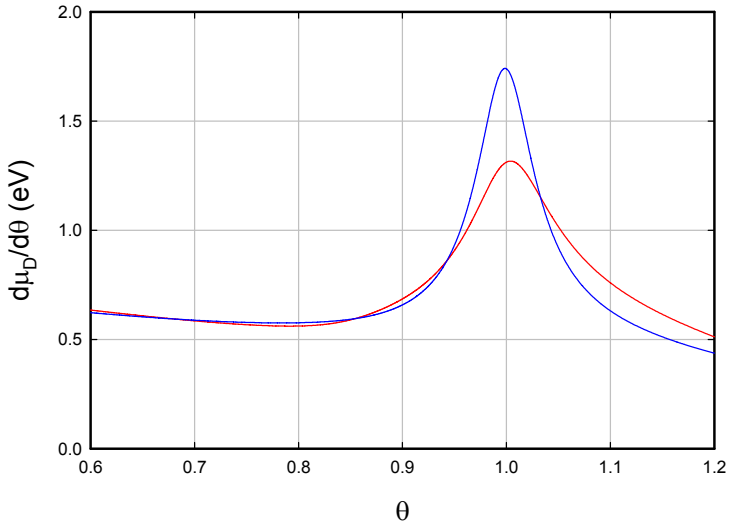

Figure 13. Slope of the model chemical potentials of Fig. 12 as a function of loading θ at 300 K.

A key issue in the construction of any empirical model is to have sufficient degrees of freedom to capture the essential features of the data of interest, and then to find sufficient experimental data so that constraints can be found for all of the different degrees of freedom. Here we were able to work with an O-site energy model taken to be quadratic in the total loading θ, and an O-site to T-site excitation energy taken to be constant or fit to available data. We introduced supplementary constraints which presume that PdH and PdD differ primarily through constant offset energies, which reduced the number of free parameters. The issue is that we have good solubility data at relatively high loading for PdH, but not for PdD. By taking the approach that we have, we are able to make use of the data for the hydride and use it to inform our model for the deuteride.

There are a number of implications of the results we obtained. For an H/Pd loading of 1 the model equilibrium pressure is 1.21 GPa, and based on the high pressure experiments of Baranowski et al. [42] this corresponds to a resistance ratio of 1.055. The corresponding value given in Crouch-Baker et al. [21] is 1.067, which is a bit higher. For a D/Pd loading of 1 the model equilibrium pressure is 1.68 GPa, which corresponds to a resistance ratio of about 1.30, which is higher than the 1.24 value corresponding to the calibration of McKubre et al. [5]. In this case the current PdH calibration slightly overestimates the loading, and the PdD calibration underestimates the loading, leading to the conclusion that the two systems are more alike than would be concluded from the standard resistance calibrations.

It is clear from this study that more experimental measurements are needed to clarify what happens at high loading, and to be sure of the assumptions and interpretations of the model. As mentioned above, it has not been unambiguously settled by experiment where hydrogen or deuterium goes once the octahedral sites are filled. If the slope of the chemical potential could be determined as a function of loading in new electrochemical experiments at very high loading, this would provide data which could be used to check for consistency with the new model, and which would provide us with an independent check on the O-site to T-site excitation energy. Additional quasi-elastic neutron diffraction experiments with PdD_x have the potential to provide direct measurements of T-site occupation, which could settle the issue. Quasi-elastic neutron scattering or NMR experiments on PdD have the potential to determine whether diffusion

in PdD occurs via an O–T–O mechanism, in contrast to PdH where the O–T–O mechanism appears to have been ruled out. Although not discussed in the text, solid state NMR experiments on PdH and PdD samples loaded above unity may help determine the site occupation of interstitials not in O-sites.

This kind of model is very powerful and can be very helpful in understanding experimental observations. We were able to develop reasonably precise estimates for the model parameters based on our interpretation of different experimental data. The value for the O-site to T-site excitation energy in PdD depends on our interpretation of resistance ratio data as a function of $\log_{10}$ fugacity in the experiments of Baranowski et al. [42]. It would be important to confirm (or else disprove) this interpretation in order to understand the resulting model better. It would also be useful to develop an equivalent plot for PdH for a similar assessment. We have relied heavily on the PdH loading measurements of Tkacz and Baranowski [65]; it would be useful to develop an equivalent data set for PdD.

Our focus has been on a model specific to 300 K. We have recently generalized our analysis to a set of isotherms at different temperatures that make up the phase diagram, with results that are compatible with the results presented in this work.

References

[1] M. Fleischmann, S. Pons and M. Hawkins, Electrochemically induced nuclear fusion of deuterium, *J. Electroanal Chem.* **201** (1989) 301; errata, **263** (1990) 187.

[2] M. Fleischmann, S. Pons, M.W. Anderson, L.J. Li and M. Hawkins, Calorimetry of the palladium–deuterium–heavy water system, *J. Electroanal. Chem.* **287** (1990) 293.

[3] P.L. Hagelstein, Bird's eye view of phonon models for excess heat in the Fleischmann–Pons experiment, *J. Cond. Mat. Nucl. Sci.* **6** 169 (2012).

[4] P.L. Hagelstein and I.U. Chaudhary, Phonon models for anomalies in condensed matter nuclear science, *Current Sci.* **108** 507 (2015).

[5] M.C.H. McKubre and F.L. Tanzella, Using resistivity to measure H/Pd and D/Pd loading: Method and significance, *Proc. ICCF12*, Yokohama, A Takahashi, K.-I. Ota and Y Iwamura (Eds.), World Scientific, Singapore, 2005, p. 392.

[6] M.C.H. McKubre, F.L. Tanzella and V. Violante, What is needed in LENR/FPE studies?, *J. Cond. Mat. Nucl. Sci.* **8** (2012) 187.

[7] M.C.H. McKubre, J. Bao, S. Crouch-Baker, P. Jayaweera, A. Sanjurjo and F. Tanzella, The palladium hydrogen system; Corrosion monitoring and energy production, it ECS Trans. **50** (2013) 357–365.

[8] M.C.H. McKubre, S. Crouch-Baker, A.M. Riley and S.I. Smedley, Excess power observations in electrochemical studies of the D/Pd system; the influence of loading, *Proc. ICCF3*, Nagoya, 1992, Nagoya, H. Ikegami (Ed.), Universal Academy Press, Tokyo, 1993, p. 5.

[9] M.C.H. McKubre, S. Crouch-Baker, R.C. Rocha-Filho, S.I. Smedley, F.L. Tanzella, T.O. Passell and J. Santucci, Isothermal flow calorimetric investigations of the D/Pd and H/Pd systems, *J. Electroanal. Chem.* **368** (1994) 55.

[10] M.C.H. McKubre, S. Crouch-Baker, A.K. Hauser, S.I. Smedley, F.L. Tanzella, M.S. Williams and S.S. Wing, Concerning reproducibility of excess power production, *Proc. 5th Int. Conf. on Cold Fusion*, 1995, pp. 17–33.

[11] T.A. Green and T.I. Quickenden, Electrolytic preparation of highly loaded deuterides of palladium, *J. Electroanaly. Chem.* **368** 121–131 (1994).

[12] M.C.H. McKubre, S. Crouch-Baker, F.L. Tanzella, S.I. Smedley, M. Williams, S. Wing, M. Maly-Schreiber, R.C. Rocha-Filho, P.C. Searson, J.G. Pronko and D.A. Kohler, Development of advanced concepts for nuclear processes in deuterated metals, Electric Power Research Institute Report TR-104195, 1994.

[13] F.L. Tanzella, S. Crouch-Baker, A. McKeown, M.C.H. McKubre, M. Williams and S. Wing, Parameters affecting the loading of hydrogen isotopes into palladium cathodes, *Proc. Sixth Int. Conf. on Cold Fusion, Progress in New Hydrogen Energy*, 1996, p. 171.

[14] T. Senjuh, H. Kamimura, T. Uehara, M. Sumi, S. Miyasita, T. Sigemitsu and N. Asami, Experimental study of electrochemical deuterium loading of Pd cathodes in the LiOD/D_2O system, *J. Alloys and Compounds* **253** (1997) 617–620.

[15] N. Asami, T. Senjuh, T. Uehara, M. Sumi, H. Kamimura and S. Miyashita, Material behavior of highly deuterated palladium, *Proc. 7th Int. Conf. on Cold Fusion*, 1998, pp. 15–21.

[16] I. Dardik, T. Zilov, H. Branover, A. El-Boher, E. Greenspan, B. Khachaturov, V. Krakov, S. Lesin, A. Shapiro and M. Tsirlin, Ultrasonically-excited electrolysis experiments at Energetics Technologies, *Proc. 14th Int. Conf. on Cold Fusion*, 2008, pp. 106–122.

[17] M. Apicella, E. Castagna, L. Capobianco, L. D'Aulerio, G. Mazzitelli, F. Sarto, A. Rosada, E. Santoro and V. Violante, Some recent results and ENEA, *Proc. 12th Int. Conf. on Cold Fusion*, 2012, pp. 117–132.

[18] V. Violante, E. Castagna, S. Lecci, F. Sarto, M. Sansovini, A. Torre, A. La Gatta, R. Duncan, G. Hubler, A. El-Boher, O. Azizi, D. Pease, D. Knies and M. McKubre, Review of materials science for studying the Fleischmann and Pons effect, *Current Sci.* **108** (2015) 540.

[19] O. Azizi, A. El-Boher, J.H. He, G.K. Hubler, D. Pease, W. Isaacson,V. Violante and S. Gangopadhyay, Progress towards understanding anomalous heat effect in metal deuterides, *Current Sci.* **108** (2015) 565.

[20] Y. Sakamoto, K. Takai, I. Takashima and M. Imada, Electrical resistance measurements as a function of composition of palladium–hydrogen (deuterium) systems by a gas phase method, *J. Phys.: Condensed Matter* **8** (1996) 3399.

[21] S. Crouch-Baker, M.C.H. McKubre and F.L. Tanzella, Variation of resistance with composition in the β-phase of the H–Pd system at 298 K, *Zeitschrift für Physikalische Chemie* **204** (1998) 247–254.

[22] P. Tripodi, M.C.H. McKubre, F.L. Tanzella, P.A. Honnor, D. Di Gioacchino, F. Celani and V. Violante, Temperature coefficient of resistivity at compositions approaching PdH, *Phys. Lett. A* **276** (2000) 122–126.

[23] P. Tripodi, D. Di Gioacchino and J.D. Vinko, AC electrical resistance measurements of PdH_x samples versus composition x, *J. Alloys and Compounds* **486** (2009) 55–59.

[24] P. Tripodi, A. Avveduto and J.D. Vinko, Strain and resistivity of PdH_x at hydrogen composition $x > 0.8$, *J. Alloys and Compounds* **500** (2010) 1–4.

[25] J. Gao, W.S. Zhang and J.J. Zhang, An explanation of hysteresis of electrical resistance—composition relationship in the Pd—H (D) and Pd alloy—H (D) systems measured by a gas phase method, *Int. J. Hydrogen Energy* **39** (2014) 21328–21334.

[26] T. Yamamoto, R. Taniguchi, T. Oka and K. Kawabata, In situ observation of deuteride formation inpalladium foil cathode by an X-ray diffraction method, *J. Less Common Metals* **172** (1991) 1381–1387.

[27] R. Felici, L. Bertalot, A. DeNinno, A. LaBarbera and V. Violante, In situ measurement of the deuterium (hydrogen) charging of a palladium electrode during electrolysis by energy dispersive X-ray diffraction, *Rev. Sci. Instr.* **66** (1995) 3344–3348.

[28] E.F. Skelton, P.L. Hagans, S.B. Qadri, D.D. Dominguez, A.C. Ehrlich and J.Z. Hu, In situ monitoring of crystallographic changes in Pd induced by diffusion of D, *Phys. Rev. B* **58** (1998) 14775.

[29] D.L. Knies, V. Violante, K.S. Grabowski, J.Z. Hu, D.D. Dominguez, J.H. He, S.B. Qadri and G.K. Hubler, In-situ synchrotron energy-dispersive X-ray diffraction study of thin Pd foils with Pd: D and Pd: H concentrations up to 1:1, *J. Appl. Phys.* **112** (2012) 083510.

[30] D. Letts and P.L. Hagelstein, Modified Szpak protocol for excess heat, *J. Cond. Matter Nucl. Sci.* **8** (2011) 1–11.

[31] P.L. Hagelstein and I.U. Chaudhary, Arguments for dideuterium near monovacancies in PdD, *15th Int. Conf. on Condensed Matter Nuclear Science*, 2009, pp. 282–287.

[32] J.E. Worsham, M.K. Wilkinson and C.G. Shull, Neutron-diffraction observations on the palladium–hydrogen and palladium–deuterium systems, *J. Phys. and Chem. Solids* **3** (1957) 303–310.

[33] G. Nelin, A neutron diffraction study of palladium hydride, *Physica status solidi (b)* **45** (1971) 527–536.

[34] H.D. Carstanjen, J.Dünstl, G.Löbl and R. Sizmann, Lattice location and determination of thermal amplitudes of deuterium in a-$PdD_{0.007}$ by channeling, *Physica Status Solidi (a)* **45** (1978) 529–536.

[35] Y. Fukai, *The Metal–Hydrogen System*, Springer, New York, 1991.

[36] J.R. Lacher, A theoretical formula for the solubility of hydrogen in palladium, *Proc. Roy. Soc. London, Series A, Math. Phys. Sci.* **161** (1937) 525–545.

[37] J.J. Rush and J.M. Rowe, Comment on High temperature thermodynamics of palladium-–hydrogen. II. Temperature dependence of partial molar properties of dilute solutions of hydrogen in the range 500—700 K [J. Chem. Phys. **65** (1976) 3915], *J. Chemical Phys.* **68** (1978) 3954–3954.

[38] M.A. Khan, J.C. Parlebas and C. Demangeat, Electronic structure and ordering of hydrogen in fcc transition metals, *J. Less Common Metals* **77** (1981) P1–P8.

[39] M.J. Gillan, A simulation model for hydrogen in palladium. I. Single-particle dynamics, *J. Phys. C: Solid State Phys.* **19** (1986) 6169.

[40] O.B. Christensen, P.D. Ditlevsen, K.W. Jacobsen, P. Stoltze, O.H. Nielsen and J.K. No, H-H interactions in Pd, *Phys. Rev. B* **40** (1989) 1993.
[41] S.M. Myers, P.M. Richards, D.M. Follstaedt and J.E. Schirber, Superstoichiometry, accelerated diffusion, and nuclear reactions in deuterium-implanted palladium, *Phys. Rev. B* **43** (1991) 9503.
[42] B. Baranowski, S.M. Filipek, M. Szustakowski, J. Farny and W. Woryna, Search for "cold-fusion" in some Me–D systems at high pressures of gaseous deuterium, *J. Less Common Metals* **158** (1990) 347–357.
[43] H. Hemmes, E. Salomons, R. Griessen, P. Sänger and A. Driessen, Lattice–gas model for the formation of palladium–silver hydrides at pressures up to 100 GPa, *Phys. Rev. B* **39** (1989) 10606.
[44] H. Sugimoto and Y. Fukai, Solubility of hydrogen in metals under high hydrogen pressures: thermodynamical calculations, *Acta Metallurgica et Materialia* **40** (1992) 2327–2336.
[45] Y. Fukai, Site preference of interstitial hydrogen in metals, *J. Less Common Metals* **101** (1984) 1–16.
[46] P.M. Richards, Molecular-dynamics investigation of deuteron separation in $PdD_{1.1}$, *Phys. Rev. B* **40** (1989) 7966.
[47] J.W. Halley and J.L. Valles, Estimate of nuclear fusion rates arising from a molecular-dynamics model of PdD_x, *Phys. Rev. B* **41** (1990) 6072.
[48] R. A. Oriani, The physical and metallurgical aspects of hydrogen in metals, *Fusion Technology* **26** 235–266 (1994).
[49] G. Benedek and P.F. Bortignon, Cold nuclear fusion: Viewpoints of solid-state physics, *Il Nuovo Cimento D* **11** (1989) 1227–1235.
[50] I.F. Silvera and F. Moshary, Deuterated palladium at temperatures from 4.3 to 400 K and pressures to 105 kbar: search for cold fusion, *Phys. Rev. B* **42** (1990) 9143.
[51] Y. Fukai and N. Okuma, Formation of superabundant vacancies in Pd hydride under high hydrogen pressures, *Phys. Rev. Lett.* **73** (1994) 1640.
[52] P.L. Hagelstein, O-site and T-site occupation of α-phase PdH_x and PdD_x, *J. Condensed Matter Nucl. Sci.* (in press).
[53] D.K. Ross, V.E. Antonov, E.L. Bokhenkov, A.I. Kolesnikov, E.G. Ponyatovsky and J. Tomkinson, Strong anisotropy in the inelastic neutron scattering from PdH at high energy transfer, *Phys. Rev. B* **58** (1998) 2591.
[54] P.L. Hagelstein Deuterium evolution reaction model and the Fleischmann–Pons experiment, *J. Condensed Matter Nucl. Sci.* **16** (2015) 46–63.
[55] P.O. Orondo, A theoretical model of interstitial hydrogen: pressure–composition–temperature, chemical potential, enthalpy and entropy, MIT Ph.D. Thesis, 2012.
[56] E. Salomons, On the lattice gas description of hydrogen in palladium: a molecular dynamics study, *J. Phys.: Condensed Matter* **2**(1990) 845.
[57] P. Orondo and P.L. Hagelstein, Basic physics model for PdH thermodynamics, *J. Condensed Matter Nucl. Sci.* **13** (2014) 149-–164.
[58] M. Ruda, E.A. Crespo and S.R. de Debiaggi, Atomistic modeling of H absorption in Pd nanoparticles, *J. Alloys and Compounds* **495** (2010) 471–475.
[59] H.C. Urey and D. Rittenberg, Some thermodynamic properties of the H1H2, H2H2 molecules and compounds containing the H2 atom, *J. Chemical Phys.* **1** (1933) 137–143.

[60] J.-M. Joubert, A calphad-type equation of state for hydrogen gas and its application to the assessment of Rh—H system, *Int. J. Hydrogen Energy* **35** (2010) 2104.
[61] J.-M. Joubert and S. Thiebaut, A thermodynamic description of the system Pd–Rh–H–D–T, *Acta Materialia* **59** (2011) 1680.
[62] P.L. Hagelstein, Equation of state and fugacity models for H_2 and for D_2, *J. Condensed Matter Nucl. Sci.* **16** (2015) 23–45.
[63] X. Ke and G.J. Kramer, Absorption and diffusion of hydrogen in palladium–silver alloys by density functional theory, *Phys. Rev. B* **66** (2002) 184304.
[64] T.B. Flanagan and W.A. Oates, The palladium–hydrogen system, *Ann. Rev. Mat. Sci.* **21** (1991) 269–304.
[65] M. Tkacz and B. Baranowski, Solubility of hydrogen in palladium hydride at high-pressure of gaseous hydrogen, *Roczniki Chemii* **50** (1976) 2159–2166.
[66] C. Elsässer, K.M. Ho, C.T. Chan and M. Fähnle, Vibrational states for hydrogen in palladium, *Phys. Rev. B* **44** (1991) 10377.
[67] P. Kamakoti and D.S. Sholl, A comparison of hydrogen diffusivities in Pd and CuPd alloys using density functional theory, *J. Membrane Sci.* **225** (2003) 145–154.
[68] S.Z. Baykara, Theoretical evaluation of diffusivity of hydrogen in palladium and rhodium, *Int. J. Hydrogen Energy* **29** (2004) 1631–1636.
[69] N. Ozawa, T.A. Roman, H. Nakanishi, H., Kasai, N.B. Arboleda Jr. and W.A. Dino, Potential energy of hydrogen atom motion on Pd (111) surface and in subsurface: A first principles calculation, *J. Appl. Phys.* **101** (2007) 123530.
[70] H. Grönbeck and V.P. Zhdanov, Effect of lattice strain on hydrogen diffusion in Pd: A density functional theory study, *Phys. Rev. B* **84** (2011) 052301.
[71] T.P. Senftle, M.J. Janik and A.C. van Duin, A reaxff investigation of hydride formation in palladium nanoclusters via monte carlo and molecular dynamics simulations, *J. Physical Chem. C* **118** (2014) 4967–4981.
[72] F.J. Rotella, J.W. Richardson Jr, L. Redey, G.P. Felcher, R.L. Hitterman and R. Kleb, Palladium deuteride formation in the cathode of an electrochemical cell, National Laboratory for High Energy Physics, KEK Report JP9206334, 1992, pp. 1–13.
[73] M.P. Pitt and E.M. Gray, Tetrahedral occupancy in the Pd–D system observed by in situ neutron powder diffraction, *EuroPhys. Lett.* **64** (2003) 344.
[74] K.G. McLennan, E.M. Gray and J.F. Dobson, Deuterium occupation of tetrahedral sites in palladium, *Phys. Rev. B* **78** (2008) 014104.
[75] M. Widenmeyer, R. Niewa, T.C. Hansen and H. Kohlmann, In situ neutron diffraction as a probe on formation and decomposition of nitrides and hydrides: A case study, *Zeitschrift für anorganische und allgemeine Chemie* **639** (2013) 285–295.
[76] J.P. Bugeat and E. Ligeon, Lattice location and trapping of hydrogen implanted in FCC metals, *Phys. Lett. A* **71** (1979) 93–96.
[77] J. Mory and E. Ligeon, Studies on dechannelling by defects and on lattice site location of hydrogen in face-centred cubic metals, *J. Materials Sci.* **17** (1982) 925–935.
[78] F. Besenbacher, B.B. Nielsen, J.K. Norskov, S.M. Myers and P. Nordlander, Interaction of hydrogen isotopes with metals: Deuterium trapped at lattice defects in palladium, *J. Fusion Energy* **9** (1990) 257–261.
[79] R.B. McLellan, The kinetic and thermodynamic effects of vacancy-interstitial interactions in Pd–H solutions, *Acta Materialia* **45** (1997) 1995–2000.
[80] F. Besenbacher, J.K. Nørskov, M.J. Puska and S. Holloway, Excitation of hydrogen motion inside a nickel vacancy, *Phys. Rev. Lett.* **55** (1985) 852.
[81] O.Y. Vekilova, D.I. Bazhanov, S.I. Simak and I.A. Abrikosov, First-principles study of vacancy-hydrogen interaction in Pd, *Phys. Rev. B* **80** (2009) 024101.
[82] J.E. Schirber and B. Morosin, Lattice constants of β–PdH_x and β-PdD_x with x near 1.0, *Phys. Rev. B* **12** (1975)117.
[83] I.S. Balbaa, P.A. Hardy, A. San-Martin, P.G. Coulter and F.D. Manchester, The effect of lattice distortions on the X-ray measurement of lattice parameters for PdH_x. I. Empirical relationships, *J. Phys. F: Metal Phys.* **17** (1987) 2041.
[84] E. Wicke and G.H. Nernst, Zustandsdiagramm und thermodynamisches Verhalten der Systeme Pd/H_2 und Pd/D_2 bei normalen Temperaturen; H/D-Trenneffekte, *Berichte der Bunsengesellschaft für physikalische Chemie* **68** (1964) 224–235.
[85] G. Sicking, Equilibrium and kinetic isotope effects, *Berichte der Bunsengesellschaft für physikalische Chemie* **76** (1972) 790–797.
[86] G. Sicking, Isotope effects in metal–hydrogen systems, *J. Less Common Metals* **101** (1984) 169–190.
[87] R.G. Leisure, L.A. Nygren and D.K. Hsu, Ultrasonic relaxation rates in palladium hydride and palladium deuteride, *Phys. Rev. B* **33** (1986) 8325.

[88] M.M. Beg and D.K. Ross, The quasielastic scattering of cold neutrons from the beta phase of palladium hydride (and hydrogen diffusion), *J. Phys. C: Solid State Phys.* **3** (1970) 2487.
[89] G. Nelin and K. Sköld, Diffusion of hydrogen in the ß-phase of Pd–H studied by small energy transfer neutron scattering, *J. Phys. and Chem. of Solids* **36** (1975) 1175–1182.
[90] D.A. Cornell and E.F.W. Seymour, Nuclear magnetic resonance study of hydrogen diffusion in palladium and palladium–cerium alloys, *J. Less Common Metals* **39** (1975) 43–54.
[91] E.F.W. Seymour, R.M. Cotts and W.D. Williams, NMR measurement of hydrogen diffusion in β–palladium hydride, *Phys. Rev. Lett.* **35** (1975) 165.
[92] P.P. Davis, E.F. W. Seymour, D. Zamir, W.D. Williams and R.M. Cotts, Nuclear magnetic resonance study of hydrogen diffusion in palladium–silver alloys, *J. Less Common Metals* **49** (1976) 159–168.
[93] P. Kamakoti and D.S. Sholl, Ab initio lattice–gas modeling of interstitial hydrogen diffusion in CuPd alloys, *Phys. Rev. B* **71** (2005) 014301.
[94] Y.M. Koroteev, O.V. Gimranova and I.P. Chernov, Hydrogen migration in palladium: First-principles calculations, *Phys. Solid State* **53** (2011) 896–900.
[95] O. Yoshinari, Origin of 'Inverse Isotope Effect' of hydrogen diffusion in palladium, In *Defect and Diffusion Forum* **312** (2011) 295–300.
[96] R. Nazarov, T. Hickel and J. Neugebauer, Ab initio study of H-vacancy interactions in fcc metals: Implications for the formation of superabundant vacancies, *Phys. Rev. B* **89** (2014) 144108.
[97] J.H. Chun and K.H. Ra, The phase-shift method for the frumkin adsorption isotherms at the Pd/H_2SO_4 and KOH solution interfaces, *J. Electrochemical Soc.* **145** (1998) 3794–3798.